Bioelectrochemistry 165 (2025) 108967

Contents lists available at ScienceDirect

Bioelectrochemistry

journal homepage: www.journals.elsevier.com/bioelectrochemistry

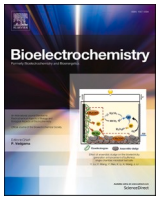

Initial quality assessment and qualitative interpretation of protein film electrochemistry catalytic data

Miriam Malagnini, Anna Aldinio-Colbachini, Laura Opdam, Andrea Di Giuliantonio, Andrea Fasano, Vincent Fourmond, Christophe Léger *

Aix Marseille Univ, CNRS, BIP, Marseille, France

ARTICLE INFO

Keywords:
Protein film electrochemistry
Direct electron transfer
Redox enzymes
Catalysis

ABSTRACT

When a redox enzyme is wired to an electrode under conditions of direct electron transfer (DET), its activity can be simply detected as a current. This approach has been reviewed extensively, but here we address a gap in the literature by discussing the initial qualitative interpretation and assessment of catalytic DET electrochemical data. Topics addressed here include electroactive coverage, turnover frequencies, mass transport limitations, film loss, redox-driven (in)activation, signal corrections, distinction between steady-state and transient responses, and identification of non-ideal behaviors. Based on our group's expertise, we provide explanations, general advice, and prescriptive guidance to help readers understand experimental issues.

1. Introduction

Various redox enzymes have been wired to electrodes, under conditions where direct electron transfer (DET) occurs. This approach enables the activity of the enzyme to be detected as a current, and offers unique advantages and challenges compared to mediated electron transfer and traditional solution assays.

Several reviews have recently been published on this topic, with a focus on various aspects of this type of experiments: the basic principles [1–3]; interfacial electron transfer kinetics, in relation to the engineering of enzymes and of electrodes [4–9]; the applications of DET in sensing [10–13] and energy [14–17]; enzymes cascades [18]; the modelling and quantitative interpretation of the electrochemical signals in terms of catalytic mechanism [19–22]; the lessons in (electro)catalysis from redox enzymes [23–26]. Macpherson and coworkers explained how potentiostats work [27] and Maisonhaute and coworkers described how to make your own, virtually for free [28].

Here we discuss the initial quality assessment and qualitative interpretation of catalytic DET electrochemical data. We shall focus on catalytic electrochemical signals obtained with redox catalysts (including enzymes) that are immobilized onto and undergo direct electron transfer with rotating electrodes. This will lead us to comment on the estimation of electroactive coverages and turnover frequencies, mass transport limitations, distinction between film loss and inactivation, signal corrections, what is the evidence for steady-state, the detection and interpretation of hysteresis, and the questions raised by the observations of unusual or non-ideal behaviors, all based on the expertise that has been acquired in our group. The text is intended to be prescriptive in some places, but it merely gives simple explanations and general advice in others. We hope that readers will recognize in this paper some of the experimental situations that they may have faced, and that our input will help them understand what may have happened, decide which experiments to run next, and interpret them.

2. The magnitude of the current

2.1. Relation between current magnitude, coverage and TOF

When a catalyst is adsorbed as a sub-monolayer onto an electrode and undergoes direct electron transfer with this electrode, the meaning of the current is very simple:

$$i = nFA\Gamma k \tag{1}$$

where A is the electrode surface and Γ is the electroactive surface coverage (in units of e.g. mol/cm^2). Only the enzyme molecules that are in electrical contact with the electrode contribute to the current and are counted in Γ. $A\Gamma$ is therefore the number of moles of enzymes wired to the electrode. k is the instant turnover frequency (TOF, in units of e.g. s^{-1}), possibly averaged over all enzyme molecules counted in $A\Gamma$. n is

* Corresponding author.
E-mail address: leger@imm.cnrs.fr (C. Léger).

https://doi.org/10.1016/j.bioelechem.2025.108967
Received 17 January 2025; Received in revised form 2 March 2025; Accepted 6 March 2025
Available online 8 March 2025

the number of electrons used or produced in one catalytic cycle, hence $nA\Gamma k$ is the number of electrons consumed or produced per second. F is the Faraday constant (10^5C/mol), i is the current (in units of Ampere, that is C/s). In this paper, we count the oxidative and reductive currents as positive and negative, respectively.

This simple expression is remarkable, because, in contrast, in most cases where the ET is *mediated* or when the catalyst *diffuses*, the current is not simply proportional to TOF.

In experiments aimed at studying a redox enzyme adsorbed onto an electrode, we strongly advocate for the use of a rotating disk electrode (RDE) [29]: spinning the disk where the enzyme is adsorbed allows controlled substrate transport towards the electrode, and makes it easier to achieve steady-state (where the current does not depend on time, scan rate and scan direction, see below). It removes the complexity that results from the substrate diffusing towards the electrode, and may uncover meaningful features that are otherwise hidden by the effect of mass transport.

The TOF value that defines the current is expected to depend on experimental conditions such as substrate and product concentrations, pH, temperature, electrode rotation rate and electrode potential, which should all always be mentioned alongside with experimental conditions of each experiment.

The major inconvenience of protein film electrochemistry (PFE) is that the electroactive coverage $A\Gamma$ is often unknown, so the TOF is not easily deduced from the current.

Depending on which type of electrode is used, the coverage $A\Gamma$ can sometimes be estimated from quartz crystal microbalance measurements [30,31], ellipsometry [32], surface plasmon resonance [33], or by the determination of the difference in enzyme concentration in the solution in contact with the electrode before and after adsorption [34]. But if the technique that is used measures the total amount of immobilized enzyme and does not differentiate between the immobilized enzyme molecules that contribute to the current and those that do not contribute to the current, then the calculated $A\Gamma$ is an overestimate (upper limit) of the amount of enzyme that actually contributes to the current, and using this value in Eq. (1) underestimates the actual TOF of the wired enzymes.

The value of $A\Gamma$ may also be measured from the magnitude of the voltammetric signals that are obtained under non-turnover conditions (where each redox site in the enzyme is supposed to give a voltammetric peak) [1], but with large enzymes these non-catalytic signals are small at best [35–37], often too small to be detected, which is unfortunate. Sometimes peaks are clearly distinguished but cannot be used to calculate coverage: this occurs e.g. when the non-catalytic signal does not report on a cofactor that is actually part of the protein [38], or when small *catalytic* signals are mistaken for non-catalytic peaks. To avoid this, it is important to confirm the non-catalytic nature of the peaks by making sure that their intensity changes in proportion to scan rate, and that they report on the cofactor actually embedded in the protein.

An upper value of the maximal coverage may be deduced from the *absence* of non-catalytic signals: it is indeed sometimes said that no non-catalytic signal can be detected above the background current if the surface coverage is lower than 1 pmol/cm^2. A *lower* limit of the TOF can then be obtained using Eq. (1) and the value of the catalytic current.

Alternatively, if the enzyme molecules spontaneously adsorb onto an electrode that is rotated into a very dilute enzyme solution (in the nM range), an upper limit of $A\Gamma$ can be deduced from the known flux of enzyme towards the RDE, and a lower value of the TOF can be deduced from the rate of change in catalytic current against time [39].

Assuming that a surface coverage as high as $\Gamma = 0.1$ pmol/cm^2 can be obtained, which is optimistic, a significant current (in the μA/cm^2 range) requires $k > 100\ s^{-1}$, which is well above the catalytic constant of most enzymes measured in solution assays [40]. This explains why the most active enzymes are the best candidates for protein film electrochemistry (PFE) studies.

However, the value of k for the enzyme on the electrode may differ from the value determined in solution assays. It is sometimes *greater* because the experimental conditions of the solution assay are not optimal, and ET between the enzyme and its soluble redox partner limits turnover (this has been reported several times, e.g. regarding CO_2 reduction by the enzyme CO-dehydrogenase [41] and H_2 oxidation by hydrogenases [35,39]). The value of k may also be smaller when the enzyme is on the electrode than in solution assays; this occurs e.g. with sulfite oxidase, probably because a conformational change that is crucial for catalysis is slower when the enzyme is adsorbed [42,43].

2.2. Dependence of the current on temperature

Enzyme activity is often very dependent on temperature (a common activation energy of 50 kJ/mol makes a rate constant increase two-fold every ten degrees) so it is very important in any kinetic experiment that the temperature be strictly controlled and its value reported.

Regarding enzyme kinetics, an advice taken from a general enzymology textbook [44] is that any temperature study should include the determination of the separate Michaelis-Menten parameters, v_m and K_M, at each temperature. Indeed, increasing the temperature may increase the maximal rate but also the Michaelis constant, and the two effects may compensate, as occurs e.g. with FeFe hydrogenases [45]; the small effect of temperature on the overall current may then be mistakenly ascribed to a very low activation energy [46].

Enzymes denature slowly upon heating, leading to bell-shaped plots of activity against temperature, but the value of the "optimum" temperature is often not meaningful because the extent of denaturation increases with the time of incubation at high temperature, and the resulting activity depends very much on details of the experimental procedures [44]. In addition, the stability of the protein film may decrease as the temperature increases.

2.3. Dependence of the catalytic current on time and potential

Assuming that the enzyme film is reasonably stable ($A\Gamma$ is nearly constant), any change in current informs on a change in TOF. This makes it possible to monitor the variations of TOF as a function of time, following a trigger: a change in potential or a change in substrate/product/inhibitor concentration, or irradiation etc. The change in current against electrode potential (E) recorded when the potential is swept is called the "waveshape", and it can be considered a fingerprint of the catalytic cycle, which encodes information about the mechanism of the enzyme. Decoding this signal is seldom straightforward [20,47].

In the simplest cases, if the catalytic response is measured in the presence of both the substrate and the product of the enzyme and under conditions of steady-state mass transport (see below), the current may vary from a low potential plateau (the intensity of which is i_{lim}^{red}) to a high potential plateau (i_{lim}^{ox}), in a sigmoidal manner (e.g. Fig. 1). A plateau is reached at a large overpotential in the limiting situation where the rates of the ET steps are very fast and do not limit turnover.

We call the enzyme "bidirectional" if it gives currents in both directions of the reactions, and "unidirectional" if the current flows in only one direction (oxidation or reduction, Fig. 1). The term "catalytic bias" is often used (at least in the hydrogenase community) to describe the ratio of the currents in the two directions. A bidirectional response may be described as "reversible" or "irreversible" depending on whether the current sharply crosses the current axis at $E = E_{eq}$ (defined by Eq. (2)), or if there is a large potential window where no activity is detected in any direction [21,25,47].

2.4. Open circuit potential

In the simultaneous presence of the oxidized substrate S of the enzyme and the reduced product P, thermodynamics imposes that the net current be zero at the equilibrium potential (Fig. 1), the value of

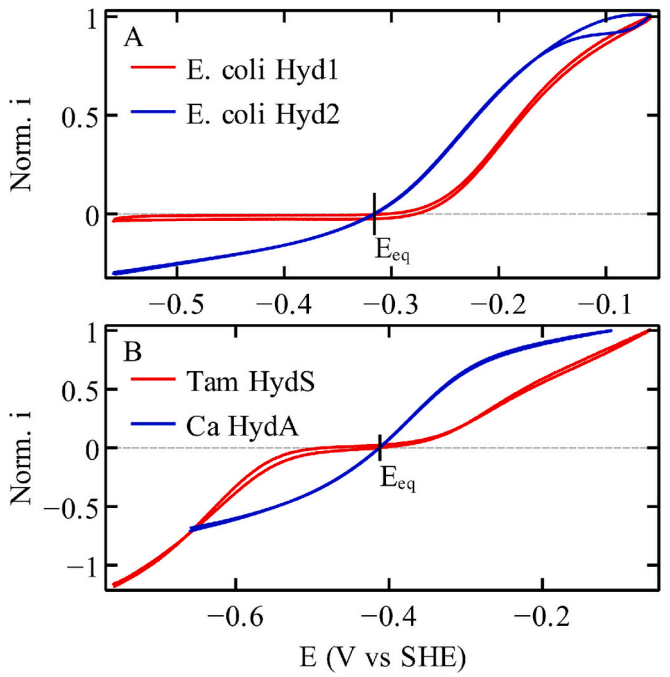

Fig. 1. Unidirectional (A, red) and bidirectional (A, blue), reversible (B, blue) and irreversible (B, red) steady-state catalytic responses. In all cases here, the positive current reveals H_2 oxidation and the negative current H_2 evolution. The CV signals have been obtained with four different hydrogenases (*Escherichia coli* NiFe hydrogenases Hyd 1 and Hyd 2, and *Thermoanaerobacter mathranii* HydS and *Clostridium acetobutylicum* HydA FeFe hydrogenases) undergoing DET with a rotating disc electrode [48,49]. The equilibrium potential calculated from the Nernst equation (Eq. (2)) is indicated. (For interpretation of the references to colour in this figure legend, the reader is referred to the web version of this article.)

which is given by the Nernst equation:

$$E_{eq} = E^{0'} + \frac{RT}{nF} log\left(\frac{[S]}{[P]}\right) \quad (2)$$

Potentiostats make it possible to measure an "open circuit potential" (OCP), the value of which is such that there is no net current.

If the electrode is covered with an enzyme whose response is bidirectional and reversible, then the OCP should equate E_{eq} (Fig. 1). This was observed in electrochemical studies of redox enzymes that reversibly convert H^+/H_2 [35,50,51] succinate/fumarate [36,52], CO_2/CO [53], CO_2/formate [54,55], NADH/NAD^+ [56], or tetrathionate/thiosulfate [57]. If the value of E_{eq} depends on pH and can be measured from the OCP, then there is no need to use a pH-meter to check the pH of the solution. The dependence of E_{eq} on pH also informs on the number of protons taken up in the reduction of S, and thus on the pKa of the substrate and product [54,55].

In contrast, if the response is bidirectional and irreversible, or if it is unidirectional, then the current is zero over a range of E values, and the value of E_{eq} cannot be measured from the OCP (Fig. 1).

2.5. Mass transport towards the RDE

When the working electrode is rotated, the solution is dragged by the spinning disk and the centrifugal force flings the solution away from the center of the electrode (Fig. 2). The solution flows from the bulk towards the electrode, resulting in convective transport of the substrate. Near the electrode the convective flow perpendicular to the electrode is zero, and in this boundary layer, the transport still occurs by diffusion, even at the highest rotation rate. However, in contrast to the situation near the surface of a stationary electrode, the size δ of the diffusion layer is

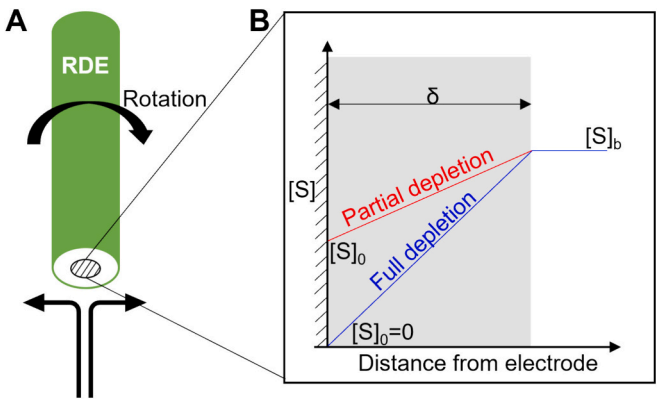

Fig. 2. The rotating disc electrode. A: The arrows indicate the rotation of the electrode and the movement of the solution. B: Substrate concentration [S] as a function of the distance from the electrode surface, showing the size of the diffusion layer (δ), and the bulk and surface concentrations ($[S]_b$ and $[S]_0$, respectively).

independent of time and electrode potential, it only depends on the electrode rotation rate [29].

Under these conditions of forced convection, the concentration of substrate remains equal to its bulk value $[S]_b$ at a distance δ from the electrode, and it decreases linearly up to a certain concentration $[S]_0$ at the interface with the electrode, as the catalytic activity of the enzyme on the electrode depletes the nearby solution (Fig. 2B).

The current that is observed equates the diffusive flux of substrate across this diffusion layer:

$$\frac{i}{A} = nFm\left([S]_b - [S]_0\right) \quad (3)$$

with

$$m = 0.62\, D^{2/3}\omega^{1/2}\, \upsilon^{-1/6} \quad (4)$$

m is the mass transport coefficient. D is the diffusion coefficient of the substrate (typically 10^{-5} cm^2/s for a small molecule), ω is the electrode rotation rate (rad/s), ν is the kinematic viscosity (typically 10^{-2} cm^2/s) [29].

The value of the maximal current that can be reached, corresponding to full substrate depletion ($[S]_0 = 0$, blue in Fig. 2B), is given by the Levich Eq. [29]:

$$i_{Levich} = nFA\, m\, [S]_b \quad (5)$$

At a rotation rate of e.g. 3 krpm (revolution/min), that is about 300 rad/s, m = 10^{-2} cm/s. With $[S]_b$ = 1 mM = 10^{-6} mol/cm^3, the mass transport limited current is in the mA/cm^2 range. This maximal current is proportional to $\omega^{1/2}$, so doubling the rotation rate should increase the current 40 % at most. Conversely, observing that the current is exactly proportional to $\omega^{1/2}$ indicates that the substrate is fully depleted at the electrode surface.

Under these conditions of extreme depletion, the current is entirely defined by the diffusion process across the diffusion layer and does not depend on $A\Gamma k$. So any change in coverage or activity is *not* reflected in a change in current. This is a very undesirable situation, because the corresponding signal bears no information about the enzyme (except that the enzyme is very active).

Even when the depletion is not complete (red in Fig. 2B), mass transport may affect the magnitude of the current. To make sure that depletion is negligible, one can verify that the measured current is well below the maximal value given by Eq. (5). Indeed, combining Eqs. (3) and (5) gives the simple relation between the observed current and the interfacial concentration of substrate:

$$[S]_0 = [S]_b \left(1 - \frac{i}{i_{Levich}}\right) \quad (6)$$

Eq. (6), shows that the depletion that is due to mass transport limitations may become crucial when the enzyme is very active (hence i is large), when the rotation is slow and when the bulk concentration is small (hence m and i_{Levich} are small). In the limit of infinitely fast rotation rate, there is no depletion, $[S]_0 = [S]_b$.

Systems other than the rotating disk electrode can also accelerate mass transport towards the electrode by convection. When an impinging jet electrode is used, the solution is forced to move towards a stationary disk electrode [58]. For the mechanistic studies we are interested in, care should be taken that the electrode surface is much smaller than the section of the nozzle so that the electrode is uniformly accessible [59,60]. We have designed a wall tube electrode (WTE) which can be 3D-printed using open-source CAD files [61], and we have derived a semi-empirical formula to calculate the mass transport coefficient m (to replace Eq. (4), all other above equations remaining correct) [60]. Higher values of m can be reached using this system than by using a RDE [62], and the analyte concentration can be changed quickly and stepwise using an appropriate mixing device [61].

Whichever system is chosen (RDE, WTE), controlled convection comes at a significant financial cost.

2.6. Koutecký–Levich approximation

The Koutecký–Levich equation (Eq. (7) below), which relates the current to the electrode rotation rate, is reminiscent of the equation giving the total conductance of a parallel circuit of resistors. The equation assumes that the value of the current is given by whichever of $nFA\Gamma k$ and i_{Levich} is the smaller.

$$\frac{1}{i} = \frac{1}{nFA\Gamma k} + \frac{1}{i_{Levich}} \quad (7)$$

Eq. (7) can be used to analyze experiments where mass transport partly limits the current. The strategy consists in obtaining $nFA\Gamma k$ by extrapolating the catalytic current to infinite flow rate or rotation rate (from the intercept on the Y axis, in a Koutecký–Levich plot of 1/i over $1/\sqrt{\omega}$, see e.g. the insets in Fig. 2 of ref. [63], or [35,64]). This is not an easy experiment, because it requires Γ to be constant during the entire experiment where the current is measured for different values of $[S]_b$ and ω, so the film must be very stable.

Eq. (7) has merit because it is simple and meaningful, but it is not strictly exact for enzyme electrocatalysis [19,65–67], because it assumes that k depends linearly on $[S]_b$ (this assumption is of course wrong for e.g. Michaelis-Menten kinetics, and using Eq. (7) leads to a systematic underestimation of the Michaelis constant [67]).

With an enzyme, substrate depletion may not be detected from the dependence of i on ω if $[S]_b$ remains much larger than the Michaelis constant, but this depletion may affect other catalytic properties. It may have an effect on the rate or extent of inhibition for example, if the substrate and the inhibitor compete [68]. As a consequence, the results of inhibition studies may be dependent on the electroactive coverage (which defines the current and the depletion) which may not be reproducible between experiments.

Another situation not accounted for by Eq. (7) is when the product inhibits the reaction: product accumulation near the electrode at low rotation rates may decrease the catalytic current [69] even if there is no significant effect of substrate depletion.

It is always simpler to use experimental conditions where the depletion is small (setting a high rotation rate of the RDE, having a bulk substrate concentration that is not too small, or even gently scratching the film to decrease the enzyme coverage, and consequently the current, if needed). Making sure that the current is at least ten times lower than the Levich value ensures that the depletion is reasonably small ($[S]_0 > 0.9\ [S]_b$). Alternatively, one can *significantly* change the rotation rate (at least two-fold), and check that the change in current is well below the change in proportion to $\omega^{1/2}$ that is expected from the Levich equation. For example, doubling the rotation rate increases the current 40 % (that is $\times\sqrt{2}$) in the worst case, where depletion is complete.

In protein film electrochemistry experiments, a large current is not the Holy Grail. If one aims at understanding how the enzyme works, it is more important to have mass transport control and stable films.

2.7. Film loss and irreversible inactivation

Relatively stable enzyme films have been made on various electrode surfaces, but in most experiments the current slowly decreases as a function of time because the surface coverage of active enzyme is not strictly constant or the enzyme inactivates over time. This is discussed with a modified version of Eq. (1):

$$i = nFA\Gamma k\, a(t) \quad (8)$$

where $a(t)$, which ranges from 0 to 1, is the time-dependent fraction of enzyme molecules that are in an active form (by "active form", we do not mean "catalytic intermediate"; any particular "active form" includes a number of catalytic intermediates, and an "inactive form" may include species that are not part of any catalytic cycle). A decrease in current may occur because the enzyme detaches from the electrode (hence Γ decreases), or because the film is stable, but some enzyme molecules irreversibly lose activity (because they denature or for other reasons, so that $a(t)$ decreases).

The comparison between the amount of enzyme that is adsorbed and the current may indicate which is the reason [30]; however, if only the current is measured, the two mechanisms that contribute to the decrease in current cannot be distinguished and are collectively described as "film loss".

Film loss can be observed by measuring the current as a function of time at a constant potential, or by regularly returning the enzyme film to standard conditions to quantify any change in current.

If film loss is slow compared to the typical timescale of the experiment, it is not a big issue on condition that all the enzymes that contribute to the current behave the same. This is a major (but often implicit) assumption when one tries to understand the meaning of PFE data (see the final section of this paper). Under this assumption, a slow film loss can be corrected a posteriori using various methods [70] (vide infra).

How film loss is affected by the electrode rotation rate and the resulting shear stress has not been investigated systematically. Immediate film loss upon rotation has been observed for the enzyme DMSO reductase [71], and also for thick polymer films containing glucose oxidase [72]. On our side, we have not seen this rotation-rate-dependent film loss with the enzymes that we studied, and unpublished data of ours suggested that an increase in shear stress does not necessarily destabilize the film, at least when the WTE is used [73].

2.8. Adsorption vs activation

It is generally assumed that any *increase* in current over time, all experimental parameters being constant, results from an activation of the enzyme (an increase in $a(t)$). However, it may happen that the electrode rotation, by favoring the convective transport of the enzyme that is in solution towards the electrode, results in its spontaneous *adsorption* from the solution (even when the concentration of enzyme in the electrochemical cell solution is in the sub-nM range [39]), and in an increase in current. The latter may be mistaken for a slow *activation* of the enzyme if one incorrectly assumes that the surface coverage is constant.

Figs. 3A, B and C show a series of voltammograms recorded with a film of the NiFe hydrogenase *E. coli* Hyd1: panel A shows the voltammogram obtained when the film is just prepared by drop casting 0.5 μL

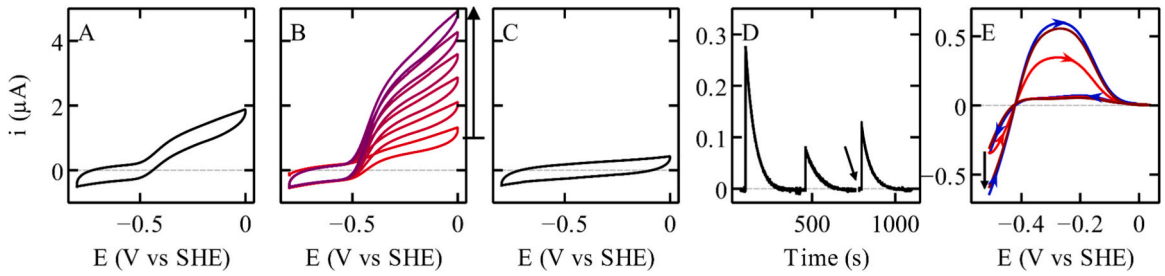

Fig. 3. Effect of enzyme adsorption and activation on the current magnitude. Panel A shows a CV for H_2 oxidation by *E. coli* NiFe hydrogenase Hyd 1 drop-casted onto a graphite RDE. B: the electrode was polished and inserted back in the same solution, the current increases over time (red to blue) because of the adsorption of the enzyme. C: when the electrode is polished again and inserted into a fresh solution with no enzyme, no signal reappears. Panel D: CO oxidation by the enzyme CO-dehydrogenase adsorbed on a graphite RDE, following the injections in the electrochemical cell of three identical aliquots of a CO solution; the positive current results from catalytic CO oxidation to CO_2. The electrode is poised at a low value at the time pointed to by the arrow, before the third injection: note the subsequent increase in current, compared to that after the 2nd injection, which indicates that the enzyme has reactivated. E: CV obtained with the FeFe hydrogenase CpIII [74] adsorbed on a graphite RDE. The first scan is shown in blue, the second in red (note the much lower magnitude), the third scan shown in a dark-red line, is preceded by a low potential poise, which reactivates the enzyme: indeed, the initial magnitude of the current is recovered. (For interpretation of the references to colour in this figure legend, the reader is referred to the web version of this article.)

of protein solution (2 μM) onto the electrode surface and letting it dry; panel B shows the response obtained after having polished the electrode with alumina powder, which is usually enough to fully removed the enzyme from the electrode surface. After polishing, one would expect to see a blank signal. However, in this case not only we do observe a catalytic current, but this current also increases scan after scan (the voltammograms are colored from red to blue, from first to last), which could be interpreted (wrongly) as the activation of enzyme molecules on the electrode that have not been removed by the polishing. This hypothesis is ruled out by the experiment in panel C, showing that the signal remains blank if the buffer in the electrochemical cell has been replaced. This observation proves that the increase in current results from some of the enzyme molecules that have detached from the initial film reabsorbing onto the polished electrode surface.

2.9. Film loss vs reversible inactivation

When the current decreases over time, it is hard to distinguish between film loss and inactivation, unless the current that has been lost (or a fraction thereof) can be recovered upon applying a specific treatment, for example a potential poise in a specific range of electrode potential [75–77]. In this case, the decrease in current is proven to result from a *reversible* inactivation process.

Many metalloenzymes reversibly (in)activate in certain potential windows. Oxidative inactivation and reductive activation were reported with e.g. NiFe hydrogenases; in that case stepping to low potential may be enough to force reactivation [75,76]. This also occurs with other enzymes. Fig. 3D shows the current resulting from CO oxidation by the enzyme CODH adsorbed onto a rotating PGE electrode [41]. In these experiments, the electrode potential is poised to a constant value, a small amount of CO-saturated solution is repeatedly injected in the cell. The first two injections give different currents, but after a negative poise at $t = 800$ s, the third injection gives a current lower than the 1st but greater than the 2nd. This indicates that not all of the current loss between the 1st and the 2nd injection was due to film loss or irreversible inactivation: some of it resulted from an inactivation process that could be reversed by the low potential poise [77].

A slightly more complex example is shown in Fig. 3E, with data obtained with the FeFe hydrogenase CpIII [74]. The positive and negative currents in this figure demonstrate catalytic H_2 oxidation and evolution. This enzyme inactivates under oxidative conditions and, like many other hydrogenases, it reactivates when the potential is swept towards low potentials. But in the case of CpIII, the current of the second voltammogram (red line) is much lower than that of the first (blue line; compare the currents at −300 mV in Fig. 3E). This may be due to film desorption during the time it takes to record the 1st CV, or to incomplete reactivation in the low potential part of the 1st CV (the hypothesis is that the reductive reactivation is too slow on the timescale of the experiment to reach completion before the potential is swept up again). Discriminating between these two hypotheses is possible by holding the potential for a few minutes at a low value in between one scan and the next one, to allow any slow reactivation to proceed. The 3rd voltammogram in Fig. 3E (dark-red line) was recorded after a few minutes poise at −560 mV, and almost 100 % of the current of the 1st voltammogram is recovered. This proves that the current decrease between the 1st and 2nd CVs was due to reversible inactivation and incomplete reactivation rather than film loss. Some FeFe hydrogenases also inactivate under reducing conditions [78], so finding a value of the electrode potential where the enzyme fully reactivates may not be straightforward.

2.10. Spikes removal and noise correction

Electrical noise from nearby devices, physical disturbance, bad electrical connections can all lead to noisy data.

The best way to deal with noise is to eliminate it at the source. Placing the electrochemical setup in a Faraday cage may help [1]. Remove all the power cables in the vicinity of the setup, try unplugging nearby devices while monitoring the signal. Unplug faulty AC to DC converters, like phone or laptop chargers or other electrical power supplies, which can be important sources of electrical noises. Potentiostats use a feedback loop to set the potential of the working electrode with respect to the reference by applying a voltage between the working and the counter electrodes; this greatly amplifies the noise on the reference electrode, so any connection issue with the reference electrode (faulty cables, dirty frits, bubbles) can be an important source of noise.

It is also sometimes possible to solve the problem ex post by processing the data after it has been recorded, as illustrated in Fig. 4.

Spikes are sudden, brief, and significant deviations from the normal signal (Fig. 4A). They may arise from faults in hardware (loose connections or faulty components) or external disturbances. They can easily be detected and removed. The open-source software QSoas [79], that we developed and made freely available for download at qsoas.org, can help you to do this and much more. Spike removal is achieved within QSoas using the commands `R` and `deldp`).

Regular noise (periodic noise of low amplitude, Fig. 4C), like that from the electrical network (50 or 60 Hz), is also easily removed on condition that its typical frequency is much larger than that of any meaningful variation in current in the signal of interest, so that damping signal variations that occur at that frequency do not distort the signal. Digital smoothing is easily performed using a Fourier transform procedure (such as that run with the command `filter-fft` in QSoas, which easily sets low-pass or band-cut filters), or a "moving average"

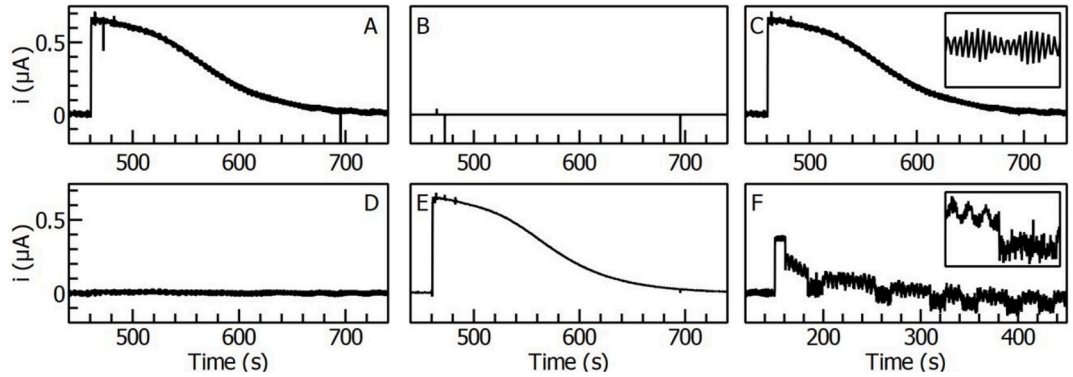

Fig. 4. Spikes and noise removal. A: the original signal. B: the spikes removed from the signal in panel A. C: The resulting signal after spike removal. D: the high frequency noise that is present in C. E: the signal after filtering C with a band cut filter to remove this high frequency noise. F: a signal with irregular fluctuations, which cannot be removed by either method. Inset shows close ups.

algorithm. All methods can lead to artifactual distortion of the data, especially near the edges, and the user should critically compare the original and smoothed signals, and make sure that the difference between the two is equally distributed across zero (Fig. 4F).

Fig. 4 exemplifies the two operations, spike removal and regular noise removal, the latter being more difficult because of the sudden change in current that one wants to retain in the filtered signal. Panel F illustrates a very difficult situation where irregular offsets in current will resist any digital filtering procedure.

2.11. Blanks and other controls

We use "blank" as a generic term to describe a negative control experiment. In cyclic voltammetry experiments, it is good practice to record and show "blank" voltammograms recorded either in the absence of enzyme or in the absence of substrate. Ideally they should be rectangular-shaped, horizontal, and flat (not showing any peak), as in Fig. 5A. Fig. 5B-E shows "blank" CVs that we consider unsatisfactory. If an unexpected peak is present in the blank, check if it is affected by electrode rotation to determine if it arises from a redox species diffusing in the solution.

In addition, to test the quality of the electrode, a blank recorded with the substrate or the inhibitor that is tested, but no enzyme, should also be examined to make sure that the direct oxidation/reduction of the substrate, or any component of the cell solution with the electrode, is not mistaken for the reaction of the enzyme.

For experiments that must be carried out at negative potential with respect to the standard hydrogen electrode, it is better to install the electrochemical setup in an anaerobic chamber (or "glove box") filled with nitrogen, although they can be expensive. Indeed, on every type of electrode material, O_2 can be reduced at a sufficiently low electrode potential, and give a reductive contribution to the current which may add to the catalytic response, and result in the formation at the electrode of reactive oxygen species which may damage the enzyme. In the experiments where we follow the activity of oxygen-sensitive enzymes after exposure to a burst of O_2 [77,80,81], we record blanks with no enzyme to make sure that this contribution is negligible. Working on CO-dehydrogenases (some of which are extremely oxygen sensitive) we recently learned the hard way that having 1 or 5 ppm of O_2 in the atmosphere of the anaerobic glove box (hence O_2 in the nM range in the solution equilibrated with that atmosphere) can make a significant difference. Traces of O_2 have arguably given rise to "pseudo" catalytic responses with immobilized glucose oxidase, and Milton et al. suggested that the exact concentration of dissolved O_2 or the exact concentration of O_2 in the anaerobic glove box used for the experiments should be reported [3].

Making sure that the catalytic response is attenuated upon addition of specific inhibitors (such as CO or cyanide for cytochrome oxidases or peroxidase [82], azide for nitrate reductase [83] or formate dehydrogenase [84], halides for multi-copper oxidases [85], etc.) is also useful to make sure that the enzyme is intact [3]. Better, the affinity for the inhibitor can be measured with the enzyme on the electrode, or the mechanism of inhibition established and then compared with the results of solution assays. Sometimes, when studying an enzyme whose native form responds on the electrode, it is possible to produce apo-enzymes [86], heat-denatured enzymes [87], or fully-inactive site-directed mutants that can be used as negative controls: they should also give no catalytic current. Milton et al. have also discussed control experiments that include product analysis, and the critical examination of the potential range where catalysis is observed [3].

Buffer components that are sometimes considered innocent may affect the biological activity of enzymes. This is the case of halides for multi-copper oxidases [85] and also FeFe hydrogenases [88]. So, comparing the results of experiments carried out in different buffers may be informative.

Irradiation, and sometimes even visible light from fluorescent lamps on the ceiling (as reported with *D. desulfuricans* FeFe hydrogenase [89,90]), may also influence the properties of certain enzymes [91,92].

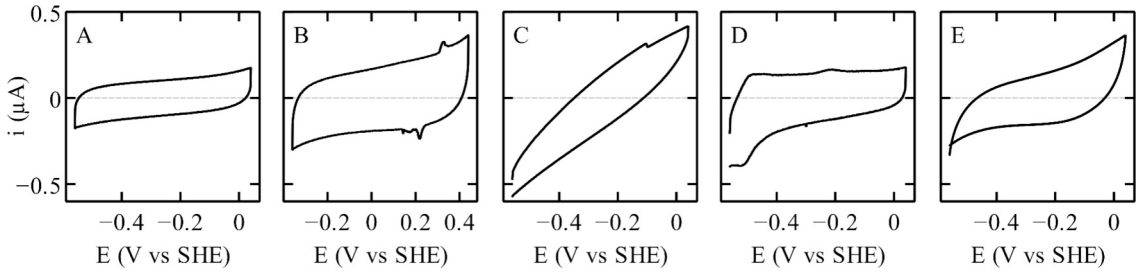

Fig. 5. Satisfactory and unsatisfactory cyclic voltammetry blanks. Only the CV shown in A is considered good: it is flat, rectangular shaped, and does not show any peak.

3. Subtraction of the capacitive current

In all experiments where the electrode potential changes (either continuously as in CV, or stepwise in CA experiments), the current that is detected is the sum of the Faradaic and capacitive contributions; the latter arises from the charging of the electrode surface (like a capacitor can be charged):

$$i = i_{Farad} + i_{cap} \tag{9}$$

This capacitive current can be recorded in an independent control experiment and then subtracted to obtain the Faradaic contribution one is interested in. Since in CV the catalytic current is proportional to the electrode surface and the scan rate, the blank should be recorded with the same electrode and at the same scan rate as the data of interest. The 2nd CV sometimes looks better than the 1st recorded after polishing. Decreasing the scan rate may be an option to decrease the contribution of the capacitive current to the overall signal. In some experiments, the contribution of the capacitive current is very small compared to the Faradaic current, so the correction is negligible.

The capacitive current and the magnitude and shape of the blanks are affected by polishing, so we recommend not to polish the electrode between the recording of the blank and the data of interest. Sometimes we record the blank before adsorbing the enzyme, without any repolishing (one of the reviewers of this paper commented that enzyme adsorption may alter the capacitive current, in contrast with what we have observed). Alternatively one may record the blank after recording the catalytic data and subsequently inactivating the enzyme film (with O_2-sensitive enzymes for example, exposure to air may be enough to remove the Faradaic contribution); sometimes one can record the capacitive current in an experiment where the enzyme is present but there is no substrate in solution.

The QSoas command to subtract one *complete* CV from another (not just one sweep from another) is `subtract /mode=indices`. When a catalytic CV is corrected by subtracting a purely capacitive blank, and if catalysis is unidirectional, then a good indication that the subtraction is satisfactory is that there is a range of potential where the current is very close to zero (for both sweep directions) (black in Fig. 6B). If the signal is bidirectional and reversible, after subtraction of the capacitive blank, the current should be zero on both sweeps at the equilibrium potential (Eq. (2)) (black in Fig. 6D), which can sometimes be measured independently (e.g. using a platinum electrode if the enzyme of interest is a hydrogenase [93]).

The voltammetric capacitive current can also be modelled (rather than measured) and then subtracted. QSoas offers various commands to do this, including the commands `baseline`, `catalytic-baseline`, `reg` and their variations. They are very flexible, and great care should therefore be taken that the data are not distorted by the subtraction of a badly modelled blank.

In potential-step experiments (discussed below), a capacitive blank can also be recorded before or after the data of interest. Potential steps produce capacitive currents that should relax exponentially towards zero. With the electrodes that we use, the typical timescale of this relaxation is in the range of seconds. Blank corrections are never perfect, so it is always very difficult to examine the details of the variations in Faradaic current that occur less than one second after a potential step. This sets a limit to the rate of the reactions triggered by potential steps that can be investigated. Decreasing the temperature may be useful to make the reactions of interest slower than the relaxation of the capacitive current. We also use potential steps of moderate amplitude (typically <200 mV) to make the capacitive contribution small enough that it can be more easily corrected. Careful examination of the blank-subtracted signal, together with knowledge about the behavior that is expected for the particular system that is studied, should indicate whether the correction is satisfactory (Fig. 6).

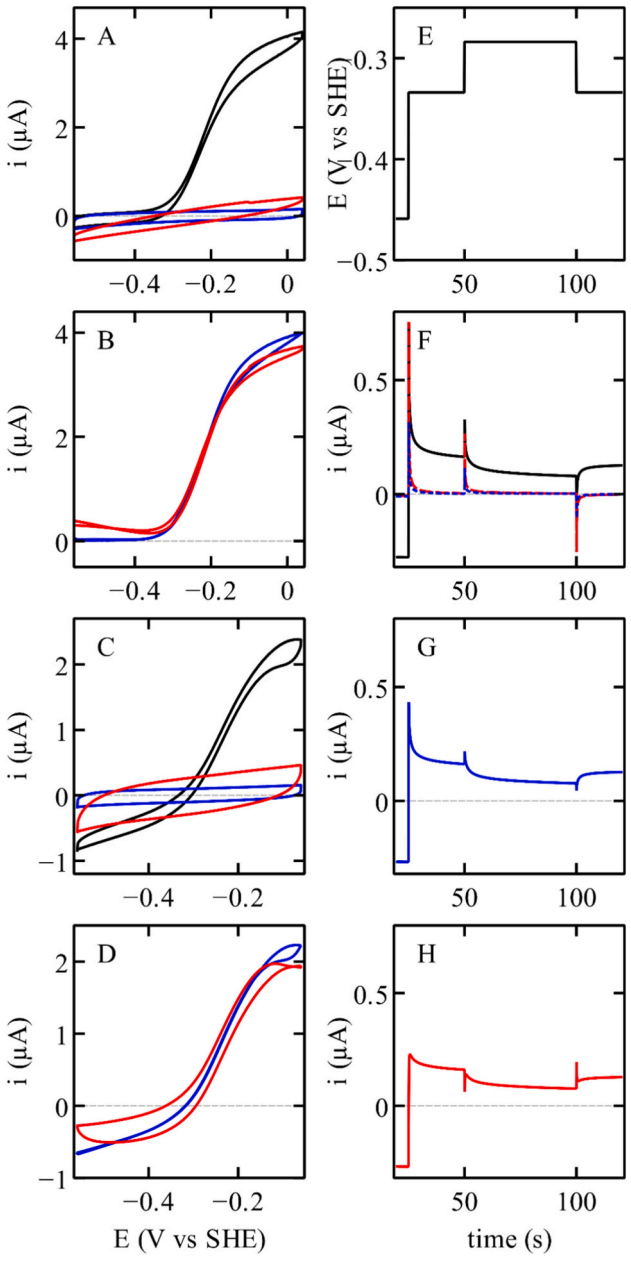

Fig. 6. Satisfactory and unsatisfactory blank subtractions from CV and CA data. A: raw voltammograms showing H_2-oxidation by a unidirectional FeFe hydrogenase (black), together with two blanks (blue and red). B: result of blank subtraction (satisfactory in blue, as deduced from the observation of a large range of potential where the Faradic current is zero, and unsatisfactory in red, with a meaningless positive current at low potential). C: raw voltammogram for H_2 oxidation and evolution by a reversible, bidirectional NiFe hydrogenase (black) and blanks (blue and red). D: result of blank subtraction (satisfactory subtraction in blue, as deduced from the fact that the current is zero on both sweeps at the equilibrium potential, and unsatisfactory in red). Panels E - H: a series of potential steps (E) lead to the CA responses shown in F, where blue and red traces are two different blanks, and the black trace is the response of a particular FeFe hydrogenase. When the blue blank is subtracted from the black trace, the blue trace in G is obtained, which we consider satisfactory: the current increases or decreases *instantly* after each step up or down, respectively, and decreases and increases *slowly* after each step up or down, respectively, as a consequence of oxidative inactivation and reductive activation. When the red blank is subtracted from the black trace, the red trace in H is obtained, which we consider unsatisfactory: the oxidative current decreases instantly at 50s after a potential step up, and increases instantly at 100 s after a step down. (For interpretation of the references to colour in this figure legend, the reader is referred to the web version of this article.)

4. Film loss correction by division and normalization

Since the Faradaic current is proportional to Γ, it is possible to obtain the pure catalytic contribution (k in Eq. (8)) by subtracting the capacitive current, then *dividing* the Faradaic current by a control signal representing the current in a different experiment where $ka(t)$ is constant, either measured in an independent control experiment, or modelled (e.g. using QSoas, using the same commands as those dedicated to baselines) [70]. The QSoas command `div` can be used to divide two signals.

The correction of film loss by dividing by an incorrectly modelled control signal can distort the data. Fig. 7A,B shows a chronoamperometry (CA) experiment that is difficult to correct for film loss, where the activity of FeFe hydrogenase is monitored after a transient exposure to CO [94]. The change in current is significantly affected by film loss, and depending on which control response is modelled (dashed lines), one may incorrectly conclude that the inhibition is fully reversible or, on the contrary, one may artificially amplify the contribution of irreversible inactivation.

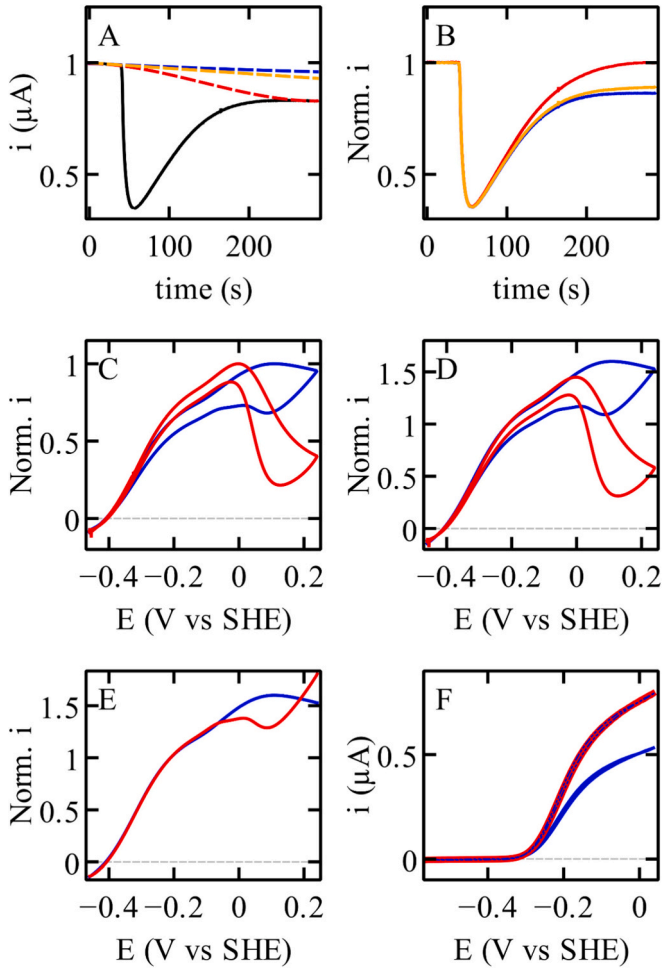

Fig. 7. Current normalization. A: raw chronoamperogram showing how an injection of an aliquot of a CO-saturated solution changes the H_2-oxidation current by a FeFe hydrogenase adsorbed onto a rotating graphite electrode (black line). The dashed lines show the modelled signals that are supposed to represent the change in current in the absence of inhibition by CO. Panel B shows the data in A corrected by division with each of the three modelled signals. C: two different CVs obtained with a particular FeFe hydrogenase, recorded under different conditions and each normalized by the maximum current: they do not overlap. D: the same two CVs as in panel C normalized by the value of the current at −210 mV vs SHE: the steady-state part of the two signals now overlap. E: two forward (blue) and backward (red) sweeps of the blue CV in panels C and D normalized by the value of the current at −210 mV vs SHE: the steady-state part of the two signals now overlap. F: the blue and red continuous lines show two different CV obtained with *E. coli* NiFe hydrogenase Hyd 1 at different enzyme coverages, while all other conditions remain the same. The dotted blue line shows the blue data after normalization so that the magnitude of the two signals is the same. The perfect overlay shows that there is no difference in shape. (For interpretation of the references to colour in this figure legend, the reader is referred to the web version of this article.)

Note that this division, or any other normalization, does not give a useful result if the current is limited by mass transport, because in that case k depends on Γ, and the current is not proportional to Γ.

Because the electroactive coverage is never fully reproducible, in order to compare signals obtained with different films or at different times, it is very useful to show CA or CV data that have been normalized by the value of the current at a certain potential, preferably a potential where the response is in a steady state, as discussed below.

5. To be or not to be in a steady state

The Faradaic contribution to the catalytic response is said to be "in a steady state" if it is independent of time. In the context of mechanistic studies, steady-state experiments are both much easier to perform and interpret (hence the century-old success of the initial-rate strategy introduced by Michaelis and Menten [95]), but much less informative than transient experiments [96,97]. In solution assays of the activity, steady-state is reached when the concentration of substrate or product changes in proportion to time, hence the rate of product formation is constant (but of course dependent on experimental conditions, including substrate concentration). In chronoamperometry (CA), steady-state implies that the current is constant (except for the decay that is due to film loss), and in cyclic voltammetry (CV) experiments, steady-state is achieved when the Faradaic current is independent of scan rate and scan direction (but the current depends on the value of the electrode potential and other experimental conditions and may also change as a result of film loss).

5.1. Steady-state catalytic chronoamperometric data

In mechanistic studies, the magnitude of the current does not really matter, because the coverage is unknown (so the actual value of the current cannot be used to determine the turnover frequency), and sometimes not very reproducible (in our hands, two-fold variations in intensity between different films are often observed and considered meaningless). But if the film is stable, experiments can be conducted to examine the *relative* change in steady-state current as a function of experimental parameters. This change in current monitored at a constant potential can easily be interpreted based on *standard steady-state kinetic models of enzyme catalysis*.

In a very common type of experiment, the electrode potential is constant and [S] is changed stepwise. The current reaches a new, constant value (in a steady-state) after each increase in substrate concentration. Slow film loss can be easily corrected (e.g. using the QSoas command `film-loss`) [70]. The change in i_{lim} against [S] at [P] = 0 for example may be Michaelien and analyzed to measure a Michaelis constant [36,63,98–100], or to observe substrate inhibition (Fig. 3 in [101]); other deviations from the Michaelien behavior may be detected [102]. Like in solution assays, K_M can only be estimated provided that the series of experiments include conditions where the enzyme is saturated with substrate ([S] ≫ K_M).

When the substrate is a gas under normal conditions, it is very easy to monitor the dependence of activity on substrate concentration in experiments where the current is measured at a constant potential while the gaseous substrate is being flushed from the electrochemical cell by a stream of a neutral gas, such as N_2. In that case, provided the electrochemical cell is open to the atmosphere of the glove box, the substrate concentration decays exactly exponentially with time, which makes kinetic modelling straightforward [103,104].

In both types of experiments, *k* in Eq. (1) depends on time because [S] evolves, but the relationship between *k* and [S] is given by a steady-state rate equation, because the enzyme adapts to a new substrate concentration on the time scale of catalysis, much faster than [S] changes with time (the typical mixing time in an electrochemical cell is about 0.1 s).

The effect of inhibitors can also be studied in the same manner. When the concentration of the inhibitor (or any other ligand that affects the signal) is changed stepwise, and a new constant current is reached instantly (e.g. Fig. 2 in ref. [84] or Fig. 8A). The effect on the activity of exponential variations in concentrations of gaseous inhibitors can also be easily interpreted when the binding/release of the inhibitor is fast and the steady-state is reached instantly (Fig. 8C) [103].

5.2. Steady-state voltammetric data

From an experimental perspective, in a voltammetric experiment, steady-state is demonstrated when, after proper subtraction of the capacitive current, the difference between the current traces recorded in the forward and backward sweeps is very small (much smaller than the current itself). This response must also be independent of scan rate.

Because of film loss, the magnitude of the signal (as opposed to its shape) may depend on time. The voltammetric responses that have different magnitudes can be compared by being overlaid after they have been normalized (division of each signal by the current measured at a certain potential) (Fig. 7F).

Steady-state may be reached in only a certain potential window in the electrochemical response (with a deviation in another potential range resulting from redox-driven inactivation, see below). In that case the forward and backward CV traces normalized by the value of the current in the potential range where steady-state is reached, may overlap even if the difference is not zero. Fig. 7D shows the overlap between two CVs normalized by the value of the current at −210 mV vs SHE, where steady state is reached. Fig. 7E shows the overlap between the forward and backward sweeps of the CV shown in blue in Fig. 7C-D, normalized by the value of the current at −210 mV vs SHE, where steady state is reached.

The change in current against electrode potential that reveals the interconversion between catalytic intermediates is expected to be in a steady-state because this interconversion occurs on the timescale of turnover, which is short compared to that of the voltammetric experiment, at least at slow scan rate [37,43]. The current quickly reaches a new steady-state when the electrode potential is changed. The steady-state response, therefore, informs on the catalytic cycle. However, remember that forced convection (towards a RDE or WTE) results in steady-state mass transport, which, if it is not efficient enough, may result in a mass-transport controlled steady-state response that is meaningless (it embeds no useful information about the enzyme).

Protein film electrochemistry adds the "potential" dimension to enzyme kinetics. The catalytic rate depends on electrode potential (in addition to all other parameters that affect the rate in solution assays: concentrations, pH, T etc.) because the catalytic cycle includes redox steps whose rate constants depend on the electrode potential. Traditional enzyme kinetics can be extended to include the dependence on electrode potential, as previously discussed (e.g. refs [19, 20, 47] and refs therein). Here, we shall only briefly describe what is expected in the simplest situations, so that one can quickly qualitatively interpret the most important voltammetric features and spot remarkable and non-ideal situations.

In some cases, in particular when the rate of electron exchange between the electrode and the enzyme is not limiting, the steady-state wave shape may be described by a combination of sigmoidal functions, which reaches well-defined values (plateau currents) at high and low potentials. When no kinetic model is available, empirical equations can be fitted to the data to measure the values of empirical parameters: the catalytic potentials E_{cat} and values of "n_{cat}" (this parameter appears in the exponential terms of the sigmoid and defines the stiffness of the sigmoid [105], a bit like the interaction coefficient in the phenomenological Hill Eq. [106]). Eq. (5) in ref. [1] is an example of such empirical electrochemical rate equation, aimed at describing a unidirectional catalytic wave in terms of three parameters: the magnitude of the current (i_{lim}), the position of the wave (E_{cat}), and its stiffness (n_{cat}). The change in E_{cat} against pH and/or substrate concentration can sometimes be simply interpreted [36,107–109].

The value of the current and the manner the current depends on the electrode potential *E* depends on the properties of the enzymes and the catalytic process, but also on the kinetics of interfacial ET (iET) between the electrode and the enzyme. As is always the case in electrochemistry, slow iET is not desirable because it broadens the signal, and shifts the catalytic response (the "wave") to higher driving force (larger overpotential). In addition to being slow, the rate of iET between electrodes and enzymes may be distributed, as a result of a distribution of enzyme orientations on the electrode. Our current understanding is that this is the reason why it is often observed that the waveshapes do not show well defined plateaus on either side, but instead show a linear increase in current with E at high or low potential (Fig. 1) [19,66,110,111]. In that case the limiting value of the current cannot be reached, but according to current models, the *slope* of the signal is proportional to the unknown limiting current [110], and, for example, the change in slope against [S] can be used to measure a Michaelis constant.

Sometimes the limitation by iET is so strong, and the rate of iET so distributed, that the sigmoidal feature of the wave disappears under a signal that looks like an exponential or a mere linear increase in current [112–114]; this result may not be a problem if the goal is to detect the activity or to obtain large and or stable currents, but it is not desirable if the goal is to use the signal to study the enzyme. Fitting a model to the data can tell whether the limitation by iET is significant [93].

Sometimes the waves show a succession of sigmoidal features, with

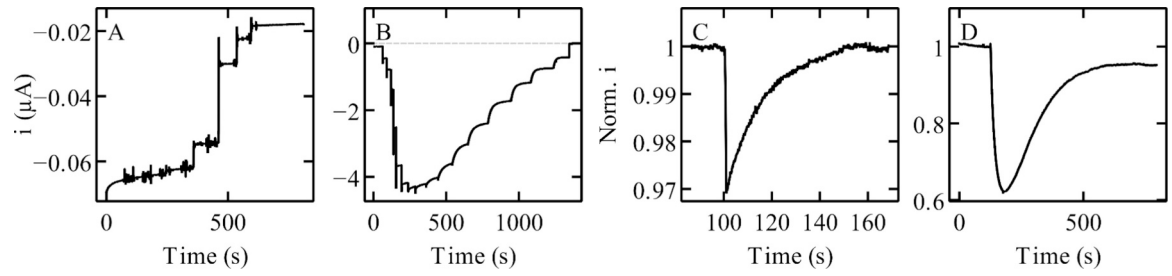

Fig. 8. Slow and fast inhibition, upon exposure of various enzymes to gaseous and non-gaseous inhibitors. Panel A: fast inhibition of nitrate reduction by periplasmic nitrate reductase upon successive injections of cyanate (unpublished). Note the instant decrease in magnitude of the reductive current each time the concentration of the inhibitor is increased stepwise. Panel B: slow substrate inhibition of nitrate reduction by periplasmic nitrate reductase upon injections of nitrate. Note the slow and exponential decrease in magnitude of the reductive current when the nitrate concentration is increased stepwise [101]. Panel C: fast CO inhibition of a NiFe hydrogenase upon transient exposure to CO [103]; Panel D: slow CO inhibition of a FeFe hydrogenase upon transient exposure to CO [94].

"boosts" (where a second sigmoidal increase in current is seen at higher overpotential than the first wave) [115–117] or attenuations of the current at high driving force (as observed with various Mo enzymes [71,83,118], cytochrome *c* nitrite reductase [119] or complex II [52]), or even combinations of both [63,102,107,120]. Empirical sigmoidal functions like those used in e.g. [71,121] may describe these more complex wave shapes.

It is important, although not straightforward, to make sure that such a complex current/potential response is not an artifact from the interaction with the electrode. The observation that the activity/potential profile shows that the enzyme is more active under conditions of lesser driving force can sometimes be mirrored (and thus confirmed) in a solution assay where the activity is monitored as a change in absorption of the redox partner over time: starting from a large excess of fully oxidized or fully reduced redox partner, the concentration of redox partner decreases over time, which is expected to slow down the reaction, but as the driving force for the reaction also decreases, it may be that the activity of the enzyme increases, leading to an acceleration of the rate before the reaction eventually stops. This was observed for fumarate reduction by complex II [122] and nitrate reduction by periplasmic nitrate reductase [123,124]. Similarly, when electrochemical experiments showed that the enzyme periplasmic nitrate reductase is inhibited by substrate but only under conditions of low reductive driving force, the observation could be confirmed by performing solution assays with different redox partners, having different reduction potentials (Fig. 4 in [101]).

5.3. Measuring the catalytic bias

There has been much interest in trying to understand what makes some redox enzymes better catalysts in one direction of the reaction than the other [25]. It may therefore be useful to quantify each enzyme's "catalytic bias" (under any particular conditions), and this can be done in various ways, which are all acceptable although not equivalent.

If the wave is sigmoidal and shows well-defined plateaus, the ratio of the limiting currents is a good metric of the catalytic bias.

$$bias = \frac{i^{ox}{}_{lim}}{i^{red}{}_{lim}} \tag{10}$$

If there are strong iET limitations and the plateaus cannot be reached, the current changes linearly with potential at high driving force and the ratio of the slopes at high and low potential gives the same information [125]. The limiting currents, the limiting slopes (the combination of parameters called "$i_{lim}/\beta d_0$") and the catalytic bias are parameters in the equations that can be fitted to the data [20].

Alternatively, the bias can be measured by examining two different experiments (performed in the presence of only substrate, or only product) [41].

A different approach is to calculate the ratio of the positive over negative current at a fixed distance δE from the equilibrium potential E_{eq} (where the current is zero) (see e.g. [126]):

$$bias = \frac{i(E_{eq} + \delta E)}{i(E_{eq} - \delta E)} \tag{11}$$

In that case the catalytic bias depends on the value of δE (since the ratio necessarily tends towards unity when δE is small). Anne K. Jones from ASU has also proposed to examine the bias in a plot of the above ratio against δE [127].

Whichever method is used, the "catalytic bias" has no intrinsic value. It depends on the concentrations of substrate/product used in the experiment that is analyzed (considering that the substrate in one direction of the reaction is the product of and may inhibit the reverse reaction) and on other experimental conditions (like pH, T etc.). This should not be surprising: the value of v_{max} for any enzyme is also dependent on the experimental conditions.

6. Deviation from steady-state in CA experiments

6.1. Slow chemical inhibition

After a stepwise change in inhibitor concentration, the new steady-state current may be reached either instantly or slowly [101,128]. The latter situation indicates that the inhibitor binds to and is released slowly from the enzyme. It may be useful here to recall that when an equilibrium between free and bound enzyme:

$$E + I \rightleftharpoons EI \tag{12}$$

relaxes towards a new equilibrium after a stepwise change in inhibitor concentration, the concentration of inhibitor-free enzyme (a(t) = [E]/([E] + [EI]) in Eq. (8)) relaxes exponentially against time, with a time constant:

$$\tau = 1/(k_i[I] + k_a) \tag{13}$$

where k_i and k_a are the 2nd- and 1st- order rate constants of inhibitor binding and release, respectively. In Eq. (13), [I] is the time-independent concentration of inhibitor after the step in inhibitor concentration (so that $k_i[I]$ is the pseudo-first order rate constant of the inhibition step) [68]. One therefore expects to see an exponential relaxation of the current with time after the step in inhibitor concentration (Fig. 8B). Note that τ in Eq. (13) should be independent of enzyme concentration, unlike the rate of catalysis and the current.

Examples of slow inhibition revealed and studied by PFE include the inhibition of fumarate reductase by oxaloacetate [129], nitrite reductase by cyanide [128], or nitrate reductase by nitrate [101] (Fig. 8B).

The effect on the activity of *exponential* variations in concentrations of gaseous inhibitors that bind slowly can also be interpreted (e.g. refs [130, 131], also Fig. 8D in [1]). In this situation, again, the change in current against time is delayed from the change in inhibitor concentration against time (Fig. 8D).

6.2. Slow, redox-driven (in)activation

The above reasoning also applies when the (in)activation is driven by a change in electrode potential, rather than the addition of inhibitor [132], as e.g. observed in voltammetric and chronoamperometry experiments carried out with hydrogenases [133,134].

Studying redox-driven (in)activations is easier in potential-steps experiments than in voltammetric experiments, because the relative change in current that reveals the change in $a(t)$ at a given potential is independent on how the steady-state activity of the active form of the enzyme, k, depends on E. So even enzymes that exhibit complex activity/potential profiles may (in)activate with a simple kinetic law.

In the simplest cases, the (in)activation that follows a potential step is first order, as observed in the hydrogenase from *A. aeolicus* [133] or periplasmic nitrate reductase [101] (Fig. 9A). This results in a mono-exponential change in current against time:

$$i(t) = i_0\, exp(-(t - t_0)/\tau) + i_\infty \tag{14}$$

where t_0 is the time of the potential step, i_0 and i_∞ the current values just after the step and after the relaxation is complete, respectively, and τ is the relaxation time:

$$\tau = 1/(k_i + k_a) \tag{15}$$

The QSoas command `fit-exponential-decay` can be used to fit Eq. (14) and measure the time constant τ. Mind that the determination of a certain value of τ is possible only if the time trace is recorded for a much longer time than the value of τ. The rate constants k_i and k_a are the (pseudo) 1st-order rate constants of activation and inactivation. They may depend on E, but not on the state of the enzyme before the potential step: this means that at a given E, irrespective of whether the enzyme inactivates or reactivates, the value of τ should be the same (Fig. 2 in ref.

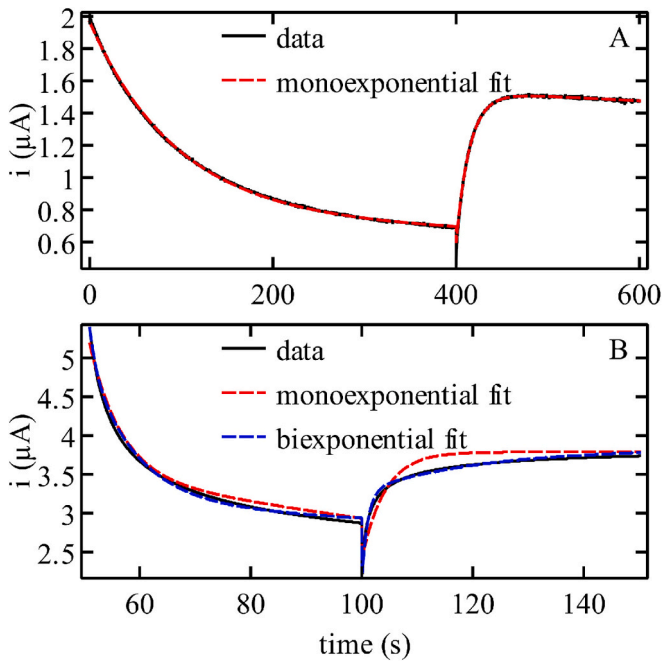

Fig. 9. Change in current observed in chronoamperometry, and resulting from redox-driven (in)activations of two distinct hydrogenases. In both experiments shown here, the current results from catalytic H_2 oxidation, the enzyme inactivates under oxidizing conditions (hence the decrease in current), and reactivates after a step to low potential (in the second part of the experiment). Panel A: the monophasic trace that reveals the (in)activation of the NiFe hydrogenase from *A. aeolicus* [133]. Panel B: the biphasic inactivation of a FeFe hydrogenase [88]. The red and blue dashed lines show the fit of mono- or biexponential functions, respectively. (For interpretation of the references to colour in this figure legend, the reader is referred to the web version of this article.)

[101]).

A complete analysis requires that the two rate constants be determined independently, which is only possible by examining not only the time constant, but also the magnitude of the relative current variation [132,133]. The QSoas command `fit-linear-kinetic-system` can help analyzing multistep chronoamperograms in order to extract the values of the (in)activation rate constants, keeping track of film loss.

The monophasic behavior may appear as biphasic because the signal is affected by film loss:

$$i(t) = [\, i_0\, exp(-(t-t_0)/\tau) + i_\infty \,] \times exp(-(t-t_0)/\tau_{loss}) \quad (16)$$

The effect of film loss may perturb the determination of the (in)activation time constant. For example when the enzyme activates slowly, the current trace may be bent down by film loss, resulting in a more pronounced curvature of the signal that is interpreted as a reactivation faster than it actually is.

More complex behaviors (resulting in multiphasic traces, e.g. Fig. 9B) are more difficult to analyze and to interpret. A multiphasic (in)activation trace may result from the contribution of more than one inactive form of the enzyme, or from the existence of various intermediates along the active to inactive reaction pathway [88,135,136].

The QSoas command `fit-exponential-decay /loss=true` can be used to fit Eq. (16). The command `fit-exponential-decay /exponentials=number` can be used to fit multiphasic traces.

6.3. Interpreting waveshapes affected by redox-driven (in)activation

Redox-driven (in)activation may give large and spectacular hysteresis in cyclic voltammetry, giving the forward and backward sweeps different shapes. If a rotating electrode is used, this hysteresis cannot be due to the diffusion of the substrate towards the electrode (in contrast to the situation where the catalyst and the substrate diffuse towards a stationary electrode). This hysteresis occurs when the value of $a(t)$ in Eq. (8) is affected by a change in potential, and when the enzyme adapts slowly to the quickly changing potential: the (in)activation process lags behind the change in electrode potential. If the voltammetry shows a hysteresis, the voltammetric shape should be dependent on scan rate.

It is often possible to conclude that the enzyme activates or inactivates in a certain range of CV by qualitatively examining the wave shape. The CV obtained with a NiFe hydrogenase in Fig. 10A is the simplest example. The current reveals H_2 oxidation by the enzyme. It increases as the electrode potential increases (and so does the driving force of the reaction). The current does not reach a plateau (for reasons discussed above). At $E > 100$ mV, the current begins to decrease. This is not due to an irreversible process (film loss, irreversible inactivation) since the shape of the backward signal clearly indicates that the enzyme reactivates when the potential is returned to a low enough value. The potential where the reactivation is very fast has been called the "switch" potential [134]. Its value is very dependent on scan rate [133,137,138]. The position of a particular feature on the voltammogram cannot be equated to a thermodynamic reduction potential if it depends on scan rate. We recommend that the latter is explored systematically and over a large range, preferentially on a logarithmic range (by examining the signals at e.g. 1 mV/s, 10 mV/s, 100 mV/s etc).

In some cases, two successive reactivations may be seen on the sweep towards low potential, indicating the oxidative formation of multiple inactive species that reactivate under less oxidative conditions; as observed e.g. with NiFeSe hydrogenase [138].

Nitrate reduction by periplasmic nitrate reductase is a slightly more complex example (see Figs. 10C and D, where the negative current is proportional to the rate of nitrate reduction) because the effect of (in)activation affects a steady-state signal that shows an extremum of activity in an intermediate window of potential (Fig. 10C). The way to read Fig. 10D is to imagine the signal after blank subtraction, to observe that the catalytic current reaches a well-defined plateau at low potential, which gives the same current value in both directions; in the intermediate range of potential, the current is smaller on the sweep downward than on the sweep upward; this implies that the enzyme inactivates at high potential. The reactivation is visible at about −200 mV, when the current magnitude increases suddenly. On the low potential plateau, the activation is complete, and on the subsequent sweep upward, one observes the catalytic response of the fully active enzyme [101].

Trace crossing, as observed in Fig. 10B and D, may be hidden by separation between the forward and backward sweeps that is caused by the capacitive current (see e.g. ref. [139]). So, it may be more visible at small scan rates where the capacitive current is small. It may be helpful to calculate the difference between the forward and backward scans, to detect any significant variation that should not occur under conditions of steady-state.

Last, trace crossing may also arise as a result of adsorption of the enzyme from the solution (hence an increase in Γ), in which case it does not reveal any activation (Fig. 10B).

7. Heterogeneity: the devil

A very important, but implicit, assumption in all of the above discussions is that all enzyme molecules that contribute to the current behave the same. On the contrary, there may be cases where distinct populations of enzymes (we are *not* speaking about distinct catalytic intermediates) behave differently and contribute to the current in an additive manner:

$$i = nFA\Gamma_1 k_1 + nFA\Gamma_2 k_2 + \ldots \quad (17)$$

where Γ_1 and Γ_2 are the two electroactive coverages.

Jeuken et al. have modelled a signal from copper-dependent nitrite

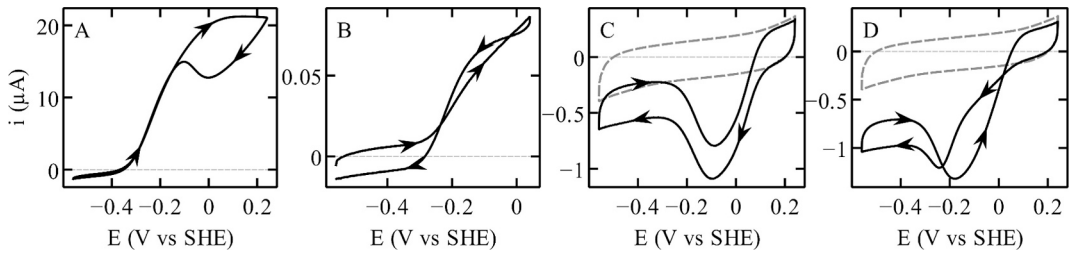

Fig. 10. Complex catalytic voltammograms. A: CV showing H_2 oxidation and evolution by *E. coli* NiFe hydrogenase Hyd 2 adsorbed on a rotating graphite electrode. Note the reversible inactivation under oxidizing conditions. B: CV obtained with *E. coli* NiFe hydrogenase Hyd 1 adsorbed on a rotating graphite electrode. The trace crossing comes from an increase in enzyme coverage upon adsorption from the solution [39]. C: steady-state CV resulting from nitrate reduction by a periplasmic nitrate reductase adsorbed on a rotating graphite electrode. Note the greater activity in the intermediate range of potential [101]. D: signal obtained with the same enzyme as in panel C, under conditions of greater nitrate concentration. The trace crossing reveals reversible oxidative inactivation [101].

reductase by summing three contributions, each characterized by a distribution of the iET rate constants around three main values, as a consequence of the trimeric structure of the enzyme [140].

We speak about "heterogeneity" when the different populations of the same enzyme film have different catalytic properties, beyond any difference in orientation and iET rates. This is a situation that one would usually want to avoid for various reasons. It may reveal that the biological sample is a mixture, maybe of a native form of the enzyme and a damaged one that still gives a catalytic response. In our experience, this makes data analysis very tricky, because the number of parameters in any model is proportional to the number of forms that contribute.

There is no definite method to identify these situations. One is to observe that the catalytic response (e.g. the steady-state wave shape) evolves from cycle to cycle, over time. We have seen this in a series of experiments where a FeFe hydrogenase was inactivated at low potential; when the potential is then swept in a range of potential where the enzyme activates, the shape of the voltammogram changes as a function of time, and could be modelled as a sum of two contributions, the relative fraction of which changes more slowly than the CV is recorded [78].

Figs. 11A and B show the unexpected changes in waveshape (after normalization) observed with different hydrogenase samples after a pH jump or freezing. In another case shown in Fig. 11C, the waveshape of a FeFe hydrogenase changed after exposure to O_2: the inactivation at high potential is not complete unless the enzyme has been exposed to O_2, indicating that possibly two different populations of the enzyme are present and one is more resistant to O_2 than the other. We have observed that the inhibition of another hydrogenase to O_2 becomes less and less pronounced after a longer exposure to O_2, as if a population of enzymes were more O_2-sensitive than the other, and eventually stopped contributing to the current, making the response of the more resistant fraction emerge more clearly.

If the enzyme is bidirectional, and if the steady-state waveshape does not change, then the catalytic bias should be constant; the observation that the bias changes (Figs. 11A and B) after a potential step, or after exposure to an inhibitor, or a pH jump may also indicate that two populations contribute.

The measurement of any change in activity with PFE is very accurate, making it very easy to detect deviations from ideal behaviors. This may be a blessing, if one can use this to learn about the enzyme, or a curse, if the only conclusion is that the sample is heterogeneous.

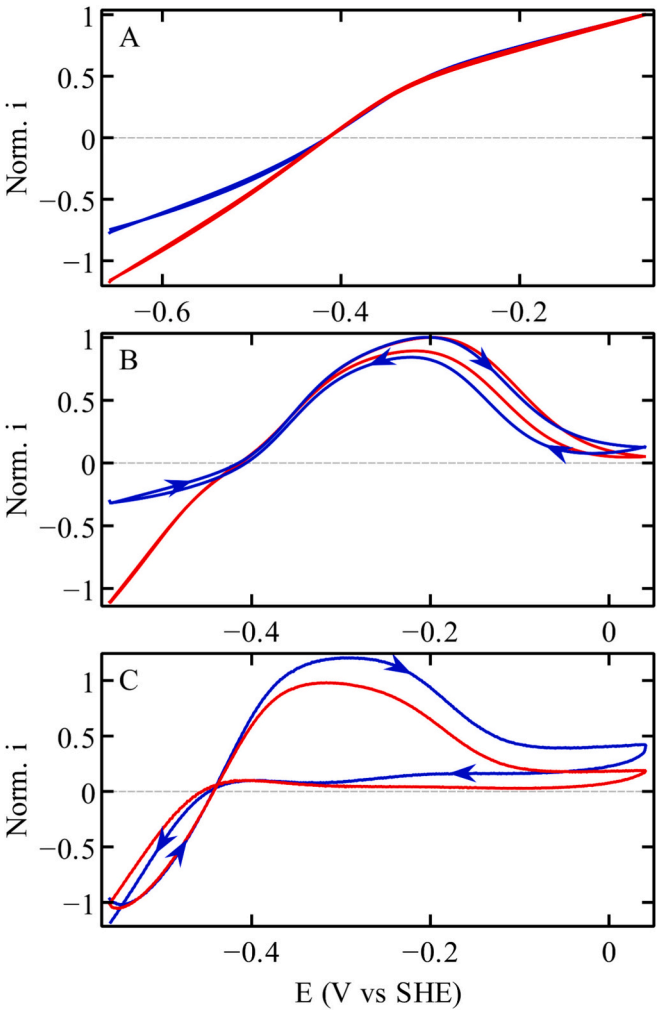

Fig. 11. Evidence for sample heterogeneity from cyclic voltammetry (unpublished data). Panel A: two catalytic responses of a particular *C. acetobutylicum* HydA1 FeFe hydrogenase sample at pH 7 [141], before (blue) and after (red) a jump to a different pH. Panel B: the voltammetric response of a cysteine-deleted mutant of the FeFe hydrogenase CpIII from *C. pasteurianum*, before (blue) and after (red) storage at −80 °C [74]. Panel C: The voltammetric response of another group B FeFe hydrogenase before (blue) and after (red) exposure to oxygen. In all cases, the two normalized voltammetric traces do not overlap like they should if all enzyme molecules on the electrode behaved the same. Note in panels A and B the clear difference in catalytic bias. (For interpretation of the references to colour in this figure legend, the reader is referred to the web version of this article.)

CRediT authorship contribution statement

Miriam Malagnini: Writing – review & editing, Writing – original draft, Data curation, Conceptualization. **Anna Aldinio-Colbachini:** Writing – review & editing, Writing – original draft, Data curation, Conceptualization. **Laura Opdam:** Writing – review & editing, Writing – original draft, Data curation, Conceptualization. **Andrea Di Giuliantonio:** Writing – review & editing, Writing – original draft, Data

curation, Conceptualization. **Andrea Fasano:** Writing – review & editing, Writing – original draft, Data curation, Conceptualization. **Vincent Fourmond:** Writing – review & editing, Writing – original draft, Data curation, Conceptualization. **Christophe Léger:** Writing – review & editing, Writing – original draft, Data curation, Conceptualization.

Declaration of competing interest

The authors declare that they have no known competing financial interests or personal relationships that could have appeared to influence the work reported in this paper.

Acknowledgements

This research was funded by the Centre National de la Recherche Scientifique, by the European Union (HORIZON-MSCA-2023-SE-01, HORIZON-EIC-2022-PATHFINDERCHALLENGES-01), Aix Marseille Université, Agence Nationale de la Recherche (ANR-21-50CE-0041, ANR-23-44CE-0046, ANR-23-SODR-0004, ANR-23-50CE-0016,), Région Sud. This work received support from the french government under the France 2030 investment plan, as part of the Initiative d'Excellence d'Aix-Marseille Université – A*MIDEX, AMX-22-RE-AB-097.

Data availability

Data will be made available on request.

References

[1] J.N. Butt, L.J.C. Jeuken, H. Zhang, J.A.J. Burton, A.L. Sutton-Cook, Protein film electrochemistry, Nature Reviews Methods Primers 3 (2023) 1–19, https://doi.org/10.1038/s43586-023-00262-7.
[2] V. Fourmond, C. Léger, Protein electrochemistry: questions and answers, Adv. Biochem. Eng. Biotechnol. 158 (2016) 1–41, https://doi.org/10.1007/10_2015_5016.
[3] R.D. Milton, S.D. Minteer, Direct enzymatic bioelectrocatalysis: differentiating between myth and reality, J. R. Soc. Interface 14 (2017), https://doi.org/10.1098/rsif.2017.0253.
[4] L.J.C. Jeuken, Structure and modification of electrode materials for protein electrochemistry, Adv. Biochem. Eng. Biotechnol. 158 (2016) 43–73, https://doi.org/10.1007/10_2015_5011.
[5] I. Mazurenko, V.P. Hitaishi, E. Lojou, Recent advances in surface chemistry of electrodes to promote direct enzymatic bioelectrocatalysis, Curr. Opin. Electrochem. 19 (2020) 113–121, https://doi.org/10.1016/j.coelec.2019.11.004.
[6] O. Smutok, T. Kavetskyy, E. Katz, Recent trends in enzyme engineering aiming to improve bioelectrocatalysis proceeding with direct electron transfer, Curr. Opin. Electrochem. 31 (2022) 100856, https://doi.org/10.1016/j.coelec.2021.100856.
[7] T. Nöll, G. Nöll, Strategies for "wiring" redox-active proteins to electrodes and applications in biosensors, biofuel cells, and nanotechnology, Chem. Soc. Rev. 40 (2011) 3564–3576, https://doi.org/10.1039/c1cs15030h.
[8] S. Shleev, J. Tkac, A. Christenson, T. Ruzgas, A.I. Yaropolov, J.W. Whittaker, L. Gorton, Direct electron transfer between copper-containing proteins and electrodes, Biosens. Bioelectron. 20 (2005) 2517–2554, https://doi.org/10.1016/j.bios.2004.10.003.
[9] U.A. Zitare, J. Szuster, D.H. Murgida, SAM-modified electrodes for understanding and harnessing the properties of redox proteins, Curr. Opin. Electrochem. 46 (2024) 101481, https://doi.org/10.1016/j.coelec.2024.101481.
[10] M.T. Meredith, S.D. Minteer, Biofuel cells: enhanced enzymatic bioelectrocatalysis, Annu Rev Anal Chem (Palo Alto, Calif) 5 (2012) 157–179, https://doi.org/10.1146/annurev-anchem-062011-143049.
[11] F. Schachinger, H. Chang, S. Scheiblbrandner, R. Ludwig, Amperometric biosensors based on direct electron transfer enzymes, Molecules 26 (2021) 4525, https://doi.org/10.3390/molecules26154525.
[12] K. Sowa, J. Okuda-Shimazaki, E. Fukawa, K. Sode, Direct electron transfer-type oxidoreductases for biomedical applications, Annu. Rev. Biomed. Eng. 26 (2024) 357–382, https://doi.org/10.1146/annurev-bioeng-110222-101926.
[13] Y. Yamashita, I. Lee, N. Loew, K. Sode, Direct electron transfer (DET) mechanism of FAD dependent dehydrogenase complexes ~from the elucidation of intra- and inter-molecular electron transfer pathway to the construction of engineered DET enzyme complexes~, Curr. Opin. Electrochem. 12 (2018) 92–100, https://doi.org/10.1016/j.coelec.2018.07.013.
[14] K.A. Vincent, A. Parkin, F.A. Armstrong, Investigating and exploiting the electrocatalytic properties of hydrogenases, Chem. Rev. 107 (2007) 4366–4413, https://doi.org/10.1021/cr050191u.
[15] S.H. Lee, D.S. Choi, S.K. Kuk, C.B. Park, Photobiocatalysis: activating redox enzymes by direct or indirect transfer of photoinduced electrons, Angew. Chem. Int. Ed. Eng. 57 (2018) 7958–7985, https://doi.org/10.1002/anie.201710070.
[16] X. Xiao, H.-Q. Xia, R. Wu, L. Bai, L. Yan, E. Magner, S. Cosnier, E. Lojou, Z. Zhu, A. Liu, Tackling the challenges of enzymatic (bio)fuel cells, Chem. Rev. 119 (2019) 9509–9558, https://doi.org/10.1021/acs.chemrev.9b00115.
[17] N. Mano, A. de Poulpiquet, O2 reduction in enzymatic biofuel cells, Chem. Rev. 118 (2018) 2392–2468, https://doi.org/10.1021/acs.chemrev.7b00220.
[18] F.A. Armstrong, B. Cheng, R.A. Herold, C.F. Megarity, B. Siritanaratkul, From protein film electrochemistry to nanoconfined enzyme cascades and the electrochemical leaf, Chem. Rev. 123 (2023) 5421–5458, https://doi.org/10.1021/acs.chemrev.2c00397.
[19] C. Léger, P. Bertrand, Direct electrochemistry of redox enzymes as a tool for mechanistic studies, Chem. Rev. 108 (2008) 2379–2438, https://doi.org/10.1021/cr0680742.
[20] V. Fourmond, C. Léger, Modelling the voltammetry of adsorbed enzymes and molecular catalysts, Curr. Opin. Electrochem. 1 (2017) 110–120, https://doi.org/10.1016/j.coelec.2016.11.002.
[21] A. Fasano, V. Fourmond, C. Léger, The difference bidirectionality makes to the kinetic modeling of molecular catalysis, Curr. Opin. Electrochem. 46 (2024) 101489, https://doi.org/10.1016/j.coelec.2024.101489.
[22] J. Hirst, Elucidating the mechanisms of coupled electron transfer and catalytic reactions by protein film voltammetry, Biochim. Biophys. Acta 1757 (2006) 225–239, https://doi.org/10.1016/j.bbabio.2006.04.002.
[23] A. Fasano, V. Fourmond, C. Léger, Outer-sphere effects on the O2 sensitivity, catalytic bias and catalytic reversibility of hydrogenases, Chem. Sci. 15 (2024) 5418–5433, https://doi.org/10.1039/d4sc00691g.
[24] F.A. Armstrong, J. Hirst, Reversibility and efficiency in electrocatalytic energy conversion and lessons from enzymes, Proc. Natl. Acad. Sci. USA 108 (2011) 14049–14054, https://doi.org/10.1073/pnas.1103697108.
[25] V. Fourmond, N. Plumeré, C. Léger, Reversible catalysis, nature reviews, Chemistry 5 (2021) 348–360, https://doi.org/10.1038/s41570-021-00268-3.
[26] L.J.C. Jeuken, D.G.H. Hetterscheid, M.T.M. Koper, C. Casadevall, C. Léger, A. Llobet, R.D. Milton, R. Nakamura, K. Tschulik, Toward an informative comparison of heterogeneous, synthetic, and biological electrocatalysis in energy conversion, Chem Catal. 4 (2024) 101098, https://doi.org/10.1016/j.checat.2024.101098.
[27] A.W. Colburn, K.J. Levey, D. O'Hare, J.V. Macpherson, Lifting the lid on the potentiostat: a beginner's guide to understanding electrochemical circuitry and practical operation, Phys. Chem. Chem. Phys. 23 (2021) 8100–8117, https://doi.org/10.1039/d1cp00661d.
[28] M. Caux, A. Achit, K. Var, G. Boitel-Aullen, D. Rose, A. Aubouy, S. Argentieri, R. Campagnolo, E. Maisonhaute, PassStat, a simple but fast, precise and versatile open source potentiostat, HardwareX 11 (2022) e00290, https://doi.org/10.1016/j.ohx.2022.e00290.
[29] A.J. Bard, L.R. Faulkner, Electrochemical Methods: Fundamentals and Applications, Wiley, 2000. https://play.google.com/store/books/details?id=kv56QgAACAAJ.
[30] K. Singh, T. McArdle, P.R. Sullivan, C.F. Blanford, Sources of activity loss in the fuel cell enzyme bilirubin oxidase, Energy Environ. Sci. 6 (2013) 2460, https://doi.org/10.1039/c3ee00043e.
[31] K. Singh, C.F. Blanford, Electrochemical quartz crystal microbalance with dissipation monitoring: a technique to optimize enzyme use in bioelectrocatalysis, ChemCatChem 6 (2014) 921–929, https://doi.org/10.1002/cctc.201300900.
[32] D. Pankratov, J. Sotres, A. Barrantes, T. Arnebrant, S. Shleev, Interfacial behavior and activity of laccase and bilirubin oxidase on bare gold surfaces, Langmuir 30 (2014) 2943–2951, https://doi.org/10.1021/la402432q.
[33] C. Gutierrez-Sanchez, A. Ciaccafava, P.Y. Blanchard, K. Monsalve, M.T. Giudici-Orticoni, S. Lecomte, E. Lojou, Efficiency of enzymatic O_2 reduction by *Myrothecium verrucaria* bilirubin oxidase probed by surface plasmon resonance, PMIRRAS, and electrochemistry, ACS Catal. 6 (2016) 5482–5492, https://doi.org/10.1021/acscatal.6b01423.
[34] I. Mazurenko, K. Monsalve, P. Infossi, M.-T. Giudici-Orticoni, F. Topin, N. Mano, E. Lojou, Impact of substrate diffusion and enzyme distribution in 3D-porous electrodes: a combined electrochemical and modelling study of a thermostable H2/O2enzymatic fuel cell, Energy Environ. Sci. 10 (2017) 1966–1982, https://doi.org/10.1039/c7ee01830d.
[35] H.R. Pershad, J.L. Duff, H.A. Heering, E.C. Duin, S.P. Albracht, F.A. Armstrong, Catalytic electron transport in Chromatium vinosum [NiFe]-hydrogenase: application of voltammetry in detecting redox-active centers and establishing that hydrogen oxidation is very fast even at potentials close to the reversible H+/H2 value, Biochemistry 38 (1999) 8992–8999, https://doi.org/10.1021/bi990108v.
[36] C. Léger, K. Heffron, H.R. Pershad, E. Maklashina, C. Luna-Chavez, G. Cecchini, B. A. Ackrell, F.A. Armstrong, Enzyme electrokinetics: energetics of succinate oxidation by fumarate reductase and succinate dehydrogenase, Biochemistry 40 (2001) 11234–11245, https://doi.org/10.1021/bi010889b.
[37] A.K. Jones, R. Camba, G.A. Reid, S.K. Chapman, F.A. Armstrong, Interruption and time-resolution of catalysis by a Flavoenzyme using fast scan protein film voltammetry, J. Am. Chem. Soc. 122 (2000) 6494–6495, https://doi.org/10.1021/ja000848n.
[38] P.N. Bartlett, F.A. Al-Lolage, There is no evidence to support literature claims of direct electron transfer (DET) for native glucose oxidase (GOx) at carbon nanotubes or graphene, J. Electroanal. Chem. (Lausanne Switz) 819 (2018) 26–37, https://doi.org/10.1016/j.jelechem.2017.06.021.
[39] A. Aldinio-Colbachini, A. Fasano, C. Guendon, A. Jacq-Bailly, J. Wozniak, C. Baffert, A. Kpebe, C. Léger, M. Brugna, V. Fourmond, Transport limited adsorption experiments give a new lower estimate of the turnover frequency of

Escherichia coli hydrogenase 1, BBA Adv. 3 (2023) 100090, https://doi.org/10.1016/j.bbadva.2023.100090.
[40] A. Bar-Even, E. Noor, Y. Savir, W. Liebermeister, D. Davidi, D.S. Tawfik, R. Milo, The moderately efficient enzyme: evolutionary and physicochemical trends shaping enzyme parameters, Biochemistry 50 (2011) 4402–4410, https://doi.org/10.1021/bi2002289.
[41] M. Benvenuti, M. Meneghello, C. Guendon, A. Jacq-Bailly, J.-H. Jeoung, H. Dobbek, C. Léger, V. Fourmond, S. Dementin, The two CO-dehydrogenases of Thermococcus sp, AM4, Biochim. Biophys. Acta Bioenerg. 1861 (2020) 148188, https://doi.org/10.1016/j.bbabio.2020.148188.
[42] S.J. Elliott, A.E. McElhaney, C. Feng, J.H. Enemark, F.A. Armstrong, A voltammetric study of interdomain electron transfer within sulfite oxidase, J. Am. Chem. Soc. 124 (2002) 11612–11613, https://doi.org/10.1021/ja027776f.
[43] T. Zeng, S. Leimkühler, U. Wollenberger, V. Fourmond, Transient catalytic voltammetry of sulfite oxidase reveals rate limiting conformational changes, J. Am. Chem. Soc. 139 (2017) 11559–11567, https://doi.org/10.1021/jacs.7b05480.
[44] A. Cornish-Bowden, Fundamentals of Enzyme Kinetics, (English Edition), 4th ed, Wiley-Blackwell, 2013.
[45] V. Fourmond, C. Baffert, K. Sybirna, S. Dementin, A. Abou-Hamdan, I. Meynial-Salles, P. Soucaille, H. Bottin, C. Léger, The mechanism of inhibition by H2 of H2-evolution by hydrogenases, Chem. Commun. 49 (2013) 6840–6842, https://doi.org/10.1039/c3cc43297a.
[46] S.V. Hexter, F. Grey, T. Happe, V. Climent, F.A. Armstrong, Electrocatalytic mechanism of reversible hydrogen cycling by enzymes and distinctions between the major classes of hydrogenases, Proc. Natl. Acad. Sci. USA 109 (2012) 11516–11521, https://doi.org/10.1073/pnas.1204770109.
[47] V. Fourmond, E.S. Wiedner, W.J. Shaw, C. Léger, Understanding and Design of Bidirectional and Reversible Catalysts of multielectron, multistep reactions, J. Am. Chem. Soc. 141 (2019) 11269–11285, https://doi.org/10.1021/jacs.9b04854.
[48] A. Fasano, C. Guendon, A. Jacq-Bailly, A. Kpebe, J. Wozniak, C. Baffert, M. D. Barrio, V. Fourmond, M. Brugna, C. Léger, A chimeric NiFe hydrogenase heterodimer to assess the role of the Electron transfer chain in tuning the Enzyme's catalytic Bias and oxygen tolerance, J. Am. Chem. Soc. 145 (2023) 20021–20030, https://doi.org/10.1021/jacs.3c06895.
[49] A. Fasano, C. Baffert, C. Schumann, G. Berggren, J.A. Birrell, V. Fourmond, C. Léger, Kinetic modeling of the reversible or irreversible electrochemical responses of FeFe-hydrogenases, J. Am. Chem. Soc. (2024), https://doi.org/10.1021/jacs.3c10693.
[50] P. Bianco, J. Haladjian, Electrocatalytic hydrogen-evolution at the pyrolytic graphite electrode in the presence of hydrogenase, J. Electrochem. Soc. 139 (1992) 2428, https://doi.org/10.1149/1.2221244.
[51] J.N. Butt, M. Filipiak, W.R. Hagen, Direct electrochemistry of Megasphaera elsdenii iron hydrogenase. Definition of the enzyme's catalytic operating potential and quantitation of the catalytic behaviour over a continuous potential range, Eur. J. Biochem. 245 (1997) 116–122, https://doi.org/10.1111/j.1432-1033.1997.00116.x.
[52] A. Sucheta, B.A. Ackrell, B. Cochran, F.A. Armstrong, Diode-like behaviour of a mitochondrial electron-transport enzyme, Nature 356 (1992) 361–362, https://doi.org/10.1038/356361a0.
[53] A. Parkin, J. Seravalli, K.A. Vincent, S.W. Ragsdale, F.A. Armstrong, Rapid and efficient electrocatalytic CO2/CO interconversions by Carboxydothermus hydrogenoformans CO dehydrogenase I on an electrode, J. Am. Chem. Soc. 129 (2007) 10328–10329, https://doi.org/10.1021/ja073643o.
[54] A. Bassegoda, C. Madden, D.W. Wakerley, E. Reisner, J. Hirst, Reversible interconversion of CO2 and formate by a molybdenum-containing formate dehydrogenase, J. Am. Chem. Soc. 136 (2014) 15473–15476, https://doi.org/10.1021/ja508647u.
[55] T. Reda, C.M. Plugge, N.J. Abram, J. Hirst, Reversible interconversion of carbon dioxide and formate by an electroactive enzyme, Proc. Natl. Acad. Sci. USA 105 (2008) 10654–10658, https://doi.org/10.1073/pnas.0801290105.
[56] Y. Zu, R.J. Shannon, J. Hirst, Reversible, electrochemical interconversion of NADH and NAD+ by the catalytic (Iambda) subcomplex of mitochondrial NADH: ubiquinone oxidoreductase (complex I), J. Am. Chem. Soc. 125 (2003) 6020–6021, https://doi.org/10.1021/ja0343961.
[57] J.M. Kurth, C. Dahl, J.N. Butt, Catalytic protein film electrochemistry provides a direct measure of the Tetrathionate/thiosulfate reduction potential, J. Am. Chem. Soc. 137 (2015) 13232–13235, https://doi.org/10.1021/jacs.5b08291.
[58] D.-T. Chin, Mass transfer to an impinging jet electrode, J. Electrochem. Soc. 125 (1978) 1461, https://doi.org/10.1149/1.2131697.
[59] W.J. Albery, S. Bruckenstein, Uniformly accessible electrodes, J. Electroanal. Chem. Interfacial Electrochem. 144 (1983) 105–112, https://doi.org/10.1016/s0022-0728(83)80148-x.
[60] A. Hadj Ahmed, J.-V. Daurelle, V. Fourmond, Optimizing the mass transport of wall-tube electrodes for protein film electrochemistry, Electrochim. Acta 403 (2022) 139521, https://doi.org/10.1016/j.electacta.2021.139521.
[61] A. Aldinio-Colbachini, A. Grossi, A.G. Duarte, J.-V. Daurelle, V. Fourmond, Combining a commercial mixer with a wall-tube electrode allows the arbitrary control of concentrations in protein film electrochemistry, Anal. Chem. 96 (2024) 4868–4875, https://doi.org/10.1021/acs.analchem.3c05293.
[62] M. Fadel, J.-V. Daurelle, V. Fourmond, J. Vicente, A new electrochemical cell with a uniformly accessible electrode to study fast catalytic reactions, Phys. Chem. Chem. Phys. 21 (2019) 12360–12371, https://doi.org/10.1039/c9cp01487j.
[63] H.C. Angove, J.A. Cole, D.J. Richardson, J.N. Butt, Protein film voltammetry reveals distinctive fingerprints of nitrite and hydroxylamine reduction by a cytochrome C nitrite reductase, J. Biol. Chem. 277 (2002) 23374–23381, https://doi.org/10.1074/jbc.M200495200.
[64] T. Meyer, F. Melin, H. Xie, I. von der Hocht, S.K. Choi, M.R. Noor, H. Michel, R. B. Gennis, T. Soulimane, P. Hellwig, Evidence for distinct electron transfer processes in terminal oxidases from different origin by means of protein film voltammetry, J. Am. Chem. Soc. 136 (2014) 10854–10857, https://doi.org/10.1021/ja505126v.
[65] H.A. Heering, J. Hirst, F.A. Armstrong, Interpreting the catalytic voltammetry of electroactive enzymes adsorbed on electrodes, J. Phys. Chem. B 102 (1998) 6889–6902, https://doi.org/10.1021/jp981023r.
[66] T. Reda, J. Hirst, Interpreting the catalytic voltammetry of an adsorbed enzyme by considering substrate mass transfer, enzyme turnover, and interfacial electron transport, J. Phys. Chem. B 110 (2006) 1394–1404, https://doi.org/10.1021/jp054783s.
[67] M. Merrouch, J. Hadj-Saïd, C. Léger, S. Dementin, V. Fourmond, Reliable estimation of the kinetic parameters of redox enzymes by taking into account mass transport towards rotating electrodes in protein film voltammetry experiments, Electrochim. Acta 245 (2017) 1059–1064, https://doi.org/10.1016/j.electacta.2017.03.114.
[68] A. Fersht, University Alan Fersht, Structure and Mechanism in Protein Science: A Guide to Enzyme Catalysis and Protein Folding, Freeman, W. H, 1999.
[69] C. Léger, A.K. Jones, W. Roseboom, S.P.J. Albracht, F.A. Armstrong, Enzyme electrokinetics: hydrogen evolution and oxidation by Allochromatium vinosum [NiFe]-hydrogenase, Biochemistry 41 (2002) 15736–15746, https://doi.org/10.1021/bi026586e.
[70] V. Fourmond, T. Lautier, C. Baffert, F. Leroux, P.-P. Liebgott, S. Dementin, M. Rousset, P. Arnoux, D. Pignol, I. Meynial-Salles, P. Soucaille, P. Bertrand, C. Léger, Correcting for electrocatalyst desorption and inactivation in chronoamperometry experiments, Anal. Chem. 81 (2009) 2962–2968, https://doi.org/10.1021/ac8025702.
[71] K. Heffron, C. Léger, R.A. Rothery, J.H. Weiner, F.A. Armstrong, Determination of an optimal potential window for catalysis by E. Coli dimethyl sulfoxide reductase and hypothesis on the role of Mo(V) in the reaction pathway, Biochemistry 40 (2001) 3117–3126, https://doi.org/10.1021/bi002452u.
[72] G. Binyamin, A. Heller, Stabilization of wired glucose oxidase anodes rotating at 1000 rpm at 37°C, J. Electrochem. Soc. 146 (1999) 2965–2967, https://doi.org/10.1149/1.1392036.
[73] A.H. Ahmed, La conception de nouvelles cellules électrochimiques pour étudier des enzymes par électrochimie directe des protéines, Ph.D. Thesis, Aix Marseille University. https://theses.fr/2022AIXM0100, 2022 (accessed December 10, 2024).
[74] A. Fasano, A. Jacq-Bailly, J. Wozniak, V. Fourmond, C. Léger, Catalytic bias and redox-driven inactivation of the group B FeFe hydrogenase CpIII, ACS Catal. 14 (2024) 7001–7010, https://doi.org/10.1021/acscatal.4c01352.
[75] S.E. Lamle, S.P.J. Albracht, F.A. Armstrong, Electrochemical potential-step investigations of the aerobic interconversions of [NiFe]-hydrogenase from Allochromatium vinosum: insights into the puzzling difference between unready and ready oxidized inactive states, J. Am. Chem. Soc. 126 (2004) 14899–14909, https://doi.org/10.1021/ja047939v.
[76] A. Abou Hamdan, B. Burlat, O. Gutiérrez-Sanz, P.-P. Liebgott, C. Baffert, A.L. De Lacey, M. Rousset, B. Guigliarelli, C. Léger, S. Dementin, O2-independent formation of the inactive states of NiFe hydrogenase, Nat. Chem. Biol. 9 (2013) 15–17, https://doi.org/10.1038/nchembio.1110.
[77] M. Merrouch, J. Hadj-Saïd, L. Domnik, H. Dobbek, C. Léger, S. Dementin, V. Fourmond, O2 inhibition of Ni-containing CO dehydrogenase is partly reversible, Chemistry 21 (2015) 18934–18938, https://doi.org/10.1002/chem.201502835.
[78] V. Hajj, C. Baffert, K. Sybirna, I. Meynial-Salles, P. Soucaille, H. Bottin, V. Fourmond, C. Léger, FeFe hydrogenase reductive inactivation and implication for catalysis, Energy Environ. Sci. 7 (2014) 715–719, https://doi.org/10.1039/C3EE42075B.
[79] V. Fourmond, QSoas: a versatile software for data analysis, Anal. Chem. 88 (2016) 5050–5052, https://doi.org/10.1021/acs.analchem.6b00224.
[80] P.-P. Liebgott, F. Leroux, B. Burlat, S. Dementin, C. Baffert, T. Lautier, V. Fourmond, P. Ceccaldi, C. Cavazza, I. Meynial-Salles, P. Soucaille, J. C. Fontecilla-Camps, B. Guigliarelli, P. Bertrand, M. Rousset, C. Léger, Relating diffusion along the substrate tunnel and oxygen sensitivity in hydrogenase, Nat. Chem. Biol. 6 (2010) 63–70, https://doi.org/10.1038/nchembio.276.
[81] A. Kubas, C. Orain, D. De Sancho, L. Saujet, M. Sensi, C. Gauquelin, I. Meynial-Salles, P. Soucaille, H. Bottin, C. Baffert, V. Fourmond, R.B. Best, J. Blumberger, C. Léger, Mechanism of O2 diffusion and reduction in FeFe hydrogenases, Nat. Chem. 9 (2017) 88–95, https://doi.org/10.1038/nchem.2592.
[82] S.J. Elliott, A.L. Bradley, D.M. Arciero, A.B. Hooper, Protonation and inhibition of Nitrosomonas europaea cytochrome c peroxidase observed with protein film voltammetry, J. Inorg. Biochem. 101 (2007) 173–179, https://doi.org/10.1016/j.jinorgbio.2006.09.009.
[83] L.J. Anderson, D.J. Richardson, J.N. Butt, Catalytic protein film voltammetry from a respiratory nitrate reductase provides evidence for complex electrochemical modulation of enzyme activity, Biochemistry 40 (2001) 11294–11307, https://doi.org/10.1021/bi002706b.
[84] W.E. Robinson, A. Bassegoda, E. Reisner, J. Hirst, Oxidation-state-dependent binding properties of the active site in a Mo-containing formate dehydrogenase, J. Am. Chem. Soc. 139 (2017) 9927–9936, https://doi.org/10.1021/jacs.7b03958.

[85] C. Vaz-Dominguez, S. Campuzano, O. Rüdiger, M. Pita, M. Gorbacheva, S. Shleev, V.M. Fernandez, A.L. De Lacey, Laccase electrode for direct electrocatalytic reduction of O2 to H2O with high-operational stability and resistance to chloride inhibition, Biosens. Bioelectron. 24 (2008) 531–537, https://doi.org/10.1016/j.bios.2008.05.002.
[86] P. Kalimuthu, P. Ringel, T. Kruse, P.V. Bernhardt, Direct electrochemistry of nitrate reductase from the fungus Neurospora crassa, Biochim. Biophys. Acta 2016 (1857) 1506–1513, https://doi.org/10.1016/j.bbabio.2016.04.001.
[87] Y. Holade, M. Yuan, R.D. Milton, D.P. Hickey, A. Sugawara, C.K. Peterbauer, D. Haltrich, S.D. Minteer, Rational combination of promiscuous enzymes yields a versatile enzymatic fuel cell with improved coulombic efficiency, J. Electrochem. Soc. 164 (2017) H3073–H3082, https://doi.org/10.1149/2.0111703jes.
[88] M. Del Barrio, M. Sensi, L. Fradale, M. Bruschi, C. Greco, L. de Gioia, L. Bertini, V. Fourmond, C. Léger, Interaction of the H-cluster of FeFe hydrogenase with halides, J. Am. Chem. Soc. 140 (2018) 5485–5492, https://doi.org/10.1021/jacs.8b01414.
[89] P. Rodríguez-Maciá, J.A. Birrell, W. Lubitz, O. Rüdiger, Electrochemical investigations on the inactivation of the [FeFe] hydrogenase from Desulfovibrio desulfuricans by O2 or light under hydrogen-producing conditions, Chempluschem 82 (2017) 540–545, https://doi.org/10.1002/cplu.201600508.
[90] S.P.J. Albracht, W. Roseboom, E.C. Hatchikian, The active site of the [FeFe]-hydrogenase from Desulfovibrio desulfuricans. I. Light sensitivity and magnetic hyperfine interactions as observed by electron paramagnetic resonance, J. Biol. Inorg. Chem. 11 (2006) 88–101, https://doi.org/10.1007/s00775-005-0039-8.
[91] M. Sensi, C. Baffert, L. Fradale, C. Gauquelin, P. Soucaille, I. Meynial-Salles, H. Bottin, L. de Gioia, M. Bruschi, V. Fourmond, C. Léger, L. Bertini, Photoinhibition of FeFe hydrogenase, ACS Catal. 7 (2017) 7378–7387, https://doi.org/10.1021/acscatal.7b02252.
[92] M. Sensi, C. Baffert, V. Fourmond, L. de Gioia, L. Bertini, C. Léger, Photochemistry and photoinhibition of the H-cluster of FeFe hydrogenases, sustain, Energy Fuel 5 (2021) 4248–4260, https://doi.org/10.1039/d1se00756d.
[93] A. Fasano, H. Land, V. Fourmond, G. Berggren, C. Léger, Reversible or irreversible catalysis of H+/H2 conversion by FeFe hydrogenases, J. Am. Chem. Soc. 143 (2021) 20320–20325, https://doi.org/10.1021/jacs.1c09554.
[94] C. Baffert, L. Bertini, T. Lautier, C. Greco, K. Sybirna, P. Ezanno, E. Etienne, P. Soucaille, P. Bertrand, H. Bottin, I. Meynial-Salles, L. De Gioia, C. Léger, CO disrupts the reduced H-cluster of FeFe hydrogenase. A combined DFT and protein film voltammetry study, J. Am. Chem. Soc. 133 (2011) 2096–2099, https://doi.org/10.1021/ja110627b.
[95] L. Michaelis, M.L. Menten, K.A. Johnson, R.S. Goody, The original Michaelis constant: translation of the, Michaelis-Menten paper, Biochemistry 50 (2011) (1913) 8264–8269, https://doi.org/10.1021/bi201284u.
[96] H.F. Fisher, Transient-state kinetic approach to mechanisms of enzymatic catalysis, Acc. Chem. Res. 38 (2005) 157–166, https://doi.org/10.1021/ar040218g.
[97] I.H. Segel, Enzyme Kinetics, John Wiley & Sons, Nashville, TN, 1993.
[98] A.L. Bradley, S.E. Chobot, D.M. Arciero, A.B. Hooper, S.J. Elliott, A distinctive electrocatalytic response from the cytochrome c peroxidase of nitrosomonas europaea, J. Biol. Chem. 279 (2004) 13297–13300, https://doi.org/10.1074/jbc.C400026200.
[99] C.F. Becker, N.J. Watmough, S.J. Elliott, Electrochemical evidence for multiple peroxidatic heme states of the diheme cytochrome c peroxidase of Pseudomonas aeruginosa, Biochemistry 48 (2009) 87–95, https://doi.org/10.1021/bi801699m.
[100] T.A. Clarke, G.L. Kemp, J.H. Van Wonderen, R.-M.A.S. Doyle, J.A. Cole, N. Tovell, M.R. Cheesman, J.N. Butt, D.J. Richardson, A.M. Hemmings, Role of a conserved glutamine residue in tuning the catalytic activity of Escherichia coli cytochrome c nitrite reductase, Biochemistry 47 (2008) 3789–3799, https://doi.org/10.1021/bi702175w.
[101] V. Fourmond, M. Sabaty, P. Arnoux, P. Bertrand, D. Pignol, C. Léger, Reassessing the strategies for trapping catalytic intermediates during nitrate reductase turnover, J. Phys. Chem. B 114 (2010) 3341–3347, https://doi.org/10.1021/jp911443y.
[102] E.T. Judd, M. Youngblut, A.A. Pacheco, S.J. Elliott, Direct electrochemistry of Shewanella oneidensis cytochrome c nitrite reductase: evidence of interactions across the dimeric interface, Biochemistry 51 (2012) 10175–10185, https://doi.org/10.1021/bi3011708.
[103] C. Léger, S. Dementin, P. Bertrand, M. Rousset, B. Guigliarelli, Inhibition and aerobic inactivation kinetics of Desulfovibrio fructosovorans NiFe hydrogenase studied by protein film voltammetry, JACS 126 (2004) 12162, https://doi.org/10.1021/ja046548d.
[104] L. Domnik, M. Merrouch, S. Goetzl, J.-H. Jeoung, C. Léger, S. Dementin, V. Fourmond, H. Dobbek, CODH-IV: a high-efficiency CO-scavenging CO dehydrogenase with resistance to O2, Angew. Chem. Int. Ed. Eng. 56 (2017) 15466–15469, https://doi.org/10.1002/anie.201709261.
[105] J.D. Gwyer, H.C. Angove, D.J. Richardson, J.N. Butt, Redox-triggered events in cytochrome c nitrite reductase, Bioelectrochemistry 63 (2004) 43–47, https://doi.org/10.1016/j.bioelechem.2003.10.013.
[106] J.N. Weiss, The hill equation revisited: uses and misuses, FASEB J. 11 (1997) 835–841, https://doi.org/10.1096/fasebj.11.11.9285481.
[107] E.T. Judd, N. Stein, A.A. Pacheco, S.J. Elliott, Hydrogen bonding networks tune proton-coupled redox steps during the enzymatic six-electron conversion of nitrite to ammonia, Biochemistry 53 (2014) 5638–5646, https://doi.org/10.1021/bi500854p.
[108] K.E. Frato, K.A. Walsh, S.J. Elliott, Functionally distinct bacterial cytochrome c peroxidases proceed through a common (electro)catalytic intermediate, Biochemistry 55 (2016) 125–132, https://doi.org/10.1021/acs.biochem.5b01162.
[109] M. Meneghello, A. Uzel, M. Broc, R.R. Manuel, A. Magalon, C. Léger, I.A. C. Pereira, A. Walburger, V. Fourmond, Electrochemical kinetics support a second coordination sphere mechanism in metal-based Formate dehydrogenase, Angew. Chem. Int. Ed. Eng. 62 (2023) e202212224, https://doi.org/10.1002/anie.202212224.
[110] C. Léger, A.K. Jones, S.P.J. Albracht, F.A. Armstrong, Effect of a dispersion of interfacial Electron transfer rates on steady state catalytic Electron transport in [NiFe]-hydrogenase and other enzymes, J. Phys. Chem. B 106 (2002) 13058–13063, https://doi.org/10.1021/jp0265687.
[111] V. Fourmond, C. Baffert, K. Sybirna, T. Lautier, A. Abou Hamdan, S. Dementin, P. Soucaille, I. Meynial-Salles, H. Bottin, C. Léger, Steady-state catalytic wave-shapes for 2-electron reversible electrocatalysts and enzymes, J. Am. Chem. Soc. 135 (2013) 3926–3938, https://doi.org/10.1021/ja311607s.
[112] R. Grinter, A. Kropp, H. Venugopal, M. Senger, J. Badley, P.R. Cabotaje, R. Jia, Z. Duan, P. Huang, S.T. Stripp, C.K. Barlow, M. Belousoff, H.S. Shafaat, G. M. Cook, R.B. Schittenhelm, K.A. Vincent, S. Khalid, G. Berggren, C. Greening, Structural basis for bacterial energy extraction from atmospheric hydrogen, Nature 615 (2023) 541–547, https://doi.org/10.1038/s41586-023-05781-7.
[113] S. Webb, A. Veliju, P. Maroni, U.-P. Apfel, T. Happe, R.D. Milton, Mesoporous electrodes enhance the electrocatalytic performance of [FeFe]-hydrogenase, Angew. Chem. Int. Ed. Eng. (2024) e202416658, https://doi.org/10.1002/anie.202416658.
[114] S. Dementin, V. Belle, P. Bertrand, B. Guigliarelli, G. Adryanczyk-Perrier, A.L. De Lacey, V.M. Fernandez, M. Rousset, C. Léger, Changing the ligation of the distal [4Fe4S] cluster in NiFe hydrogenase impairs inter- and intramolecular electron transfers, J. Am. Chem. Soc. 128 (2006) 5209–5218, https://doi.org/10.1021/ja060233b.
[115] J.M. Hudson, K. Heffron, V. Kotlyar, Y. Sher, E. Maklashina, G. Cecchini, F. A. Armstrong, Electron transfer and catalytic control by the iron-sulfur clusters in a respiratory enzyme, E. Coli fumarate reductase, J. Am. Chem. Soc. 127 (2005) 6977–6989, https://doi.org/10.1021/ja043404q.
[116] J.N. Butt, J. Thornton, D.J. Richardson, P.S. Dobbin, Voltammetry of a flavocytochrome c3: the lowest potential heme modulates fumarate reduction rates, Biophys. J. 78 (2000) 1001–1009, https://doi.org/10.1016/s0006-3495(00)76658-6.
[117] K.E. Ellis, J. Seidel, O. Einsle, S.J. Elliott, Geobacter sulfurreducens cytochrome c peroxidases: electrochemical classification of catalytic mechanisms, Biochemistry 50 (2011) 4513–4520, https://doi.org/10.1021/bi200399h.
[118] B. Frangioni, P. Arnoux, M. Sabaty, D. Pignol, P. Bertrand, B. Guigliarelli, C. Léger, In Rhodobacter sphaeroides respiratory nitrate reductase, the kinetics of substrate binding favors intramolecular electron transfer, J. Am. Chem. Soc. 126 (2004) 1328–1329, https://doi.org/10.1021/ja0384072.
[119] J.D. Gwyer, D.J. Richardson, J.N. Butt, Diode or tunnel-diode characteristics? Resolving the catalytic consequences of proton coupled electron transfer in a multi-centered oxidoreductase, J. Am. Chem. Soc. 127 (2005) 14964–14965, https://doi.org/10.1021/ja054160s.
[120] S.J. Elliott, K.R. Hoke, K. Heffron, M. Palak, R.A. Rothery, J.H. Weiner, F. A. Armstrong, Voltammetric studies of the catalytic mechanism of the respiratory nitrate reductase from Escherichia coli: how nitrate reduction and inhibition depend on the oxidation state of the active site, Biochemistry 43 (2004) 799–807, https://doi.org/10.1021/bi035869j.
[121] J. Hirst, A. Sucheta, B.A.C. Ackrell, F.A. Armstrong, Electrocatalytic voltammetry of succinate dehydrogenase: direct quantification of the catalytic properties of a complex electron-transport enzyme, J. Am. Chem. Soc. 118 (1996) 5031–5038, https://doi.org/10.1021/ja9534361.
[122] B.A. Ackrell, F.A. Armstrong, B. Cochran, A. Sucheta, T. Yu, Classification of fumarate reductases and succinate dehydrogenases based upon their contrasting behaviour in the reduced benzylviologen/fumarate assay, FEBS Lett. 326 (1993) 92–94, https://doi.org/10.1016/0014-5793(93)81768-u.
[123] V. Fourmond, B. Burlat, S. Dementin, M. Sabaty, P. Arnoux, E. Etienne, B. Guigliarelli, P. Bertrand, D. Pignol, C. Léger, Dependence of catalytic activity on driving force in solution assays and protein film voltammetry: insights from the comparison of nitrate reductase mutants, Biochemistry 49 (2010) 2424–2432, https://doi.org/10.1021/bi902140e.
[124] A.J. Gates, D.J. Richardson, J.N. Butt, Voltammetric characterization of the aerobic energy-dissipating nitrate reductase of Paracoccus pantotrophus: exploring the activity of a redox-balancing enzyme as a function of electrochemical potential, Biochem. J. 409 (2008) 159–168, https://doi.org/10.1042/BJ20071088.
[125] P. Ceccaldi, K. Schuchmann, V. Müller, S.J. Elliott, The hydrogen dependent CO2 reductase: the first completely CO tolerant FeFe-hydrogenase, Energy Environ. Sci. 10 (2017) 503–508, https://doi.org/10.1039/c6ee02494g.
[126] J.M. Kurth, J.N. Butt, D.J. Kelly, C. Dahl, Influence of haem environment on the catalytic properties of the tetrathionate reductase TsdA from campylobacter jejuni, Biosci. Rep. 36 (2016) e00422, https://doi.org/10.1042/BSR20160457.
[127] A.K. Jones, International Conference on Hydrogenases and other redox biocatalysts for energy conversion (ICH) #13 (2023).
[128] J.D. Gwyer, D.J. Richardson, J.N. Butt, Resolving complexity in the interactions of redox enzymes and their inhibitors: contrasting mechanisms for the inhibition of a cytochrome c nitrite reductase revealed by protein film voltammetry, Biochemistry 43 (2004) 15086–15094, https://doi.org/10.1021/bi049085x.
[129] H.A. Heering, J.H. Weiner, F.A. Armstrong, Direct detection and measurement of Electron relays in a multicentered enzyme: voltammetry of electrode-surface films

of E. Coli fumarate reductase, an Iron−sulfur Flavoprotein, J. Am. Chem. Soc. 119 (1997) 11628–11638, https://doi.org/10.1021/ja9723242.
[130] F. Leroux, S. Dementin, B. Burlat, L. Cournac, A. Volbeda, S. Champ, L. Martin, B. Guigliarelli, P. Bertrand, J. Fontecilla-Camps, M. Rousset, C. Léger, Experimental approaches to kinetics of gas diffusion in hydrogenase, Proc. Natl. Acad. Sci. USA 105 (2008) 11188–11193, https://doi.org/10.1073/pnas.0803689105.
[131] M.G. Almeida, C.M. Silveira, B. Guigliarelli, P. Bertrand, J.J.G. Moura, I. Moura, C. Léger, A needle in a haystack: the active site of the membrane-bound complex cytochrome c nitrite reductase, FEBS Lett. 581 (2007) 284–288, https://doi.org/10.1016/j.febslet.2006.12.023.
[132] M. Barrio, V. Fourmond, Redox (in)activations of Metalloenzymes: a protein film voltammetry approach, ChemElectroChem 6 (2019) 4949–4962, https://doi.org/10.1002/celc.201901028.
[133] V. Fourmond, P. Infossi, M.-T. Giudici-Orticoni, P. Bertrand, C. Léger, Chronoamperometric method for studying the anaerobic inactivation of an oxygen tolerant NiFe hydrogenase, J. Am. Chem. Soc. 132 (2010) 4848–4857, https://doi.org/10.1021/ja910685j.
[134] A.K. Jones, S.E. Lamle, H.R. Pershad, K.A. Vincent, S.P.J. Albracht, F. A. Armstrong, Enzyme electrokinetics: electrochemical studies of the anaerobic interconversions between active and inactive states of Allochromatium vinosum [NiFe]-hydrogenase, J. Am. Chem. Soc. 125 (2003) 8505–8514, https://doi.org/10.1021/ja035296y.
[135] M. Winkler, J. Duan, A. Rutz, C. Felbek, L. Scholtysek, O. Lampret, J. Jaenecke, U.-P. Apfel, G. Gilardi, F. Valetti, V. Fourmond, E. Hofmann, C. Léger, T. Happe, A safety cap protects hydrogenase from oxygen attack, Nat. Commun. 12 (2021) 756, https://doi.org/10.1038/s41467-020-20861-2.
[136] V. Fourmond, C. Greco, K. Sybirna, C. Baffert, P.-H. Wang, P. Ezanno, M. Montefiori, M. Bruschi, I. Meynial-Salles, P. Soucaille, J. Blumberger, H. Bottin, L. De Gioia, C. Léger, The oxidative inactivation of FeFe hydrogenase reveals the flexibility of the H-cluster, Nat. Chem. 6 (2014) 336–342, https://doi.org/10.1038/nchem.1892.
[137] A. Abou Hamdan, P.-P. Liebgott, V. Fourmond, O. Gutiérrez-Sanz, A.L. De Lacey, P. Infossi, M. Rousset, S. Dementin, C. Léger, Relation between anaerobic inactivation and oxygen tolerance in a large series of NiFe hydrogenase mutants, Proc. Natl. Acad. Sci. USA 109 (2012) 19916–19921, https://doi.org/10.1073/pnas.1212258109.
[138] P. Ceccaldi, M.C. Marques, V. Fourmond, I.C. Pereira, C. Léger, Oxidative inactivation of NiFeSe hydrogenase, Chem. Commun. 51 (2015) 14223–14226, https://doi.org/10.1039/c5cc05930e.
[139] M. Dagys, A. Laurynėnas, D. Ratautas, J. Kulys, R. Vidžiūnaitė, M. Talaikis, G. Niaura, L. Marcinkevičienė, R. Meškys, S. Shleev, Oxygen electroreduction catalysed by laccase wired to gold nanoparticles via the trinuclear copper cluster, Energy Environ. Sci. 10 (2017) 498–502, https://doi.org/10.1039/c6ee02232d.
[140] H.J. Wijma, L.J.C. Jeuken, M.P. Verbeet, F.A. Armstrong, G.W. Canters, Protein film voltammetry of copper-containing nitrite reductase reveals reversible inactivation, J. Am. Chem. Soc. 129 (2007) 8557–8565, https://doi.org/10.1021/ja071274q.
[141] C. Baffert, M. Demuez, L. Cournac, B. Burlat, B. Guigliarelli, P. Bertrand, L. Girbal, C. Léger, Hydrogen-activating enzymes: activity does not correlate with oxygen sensitivity, Angew. Chem. Int. Ed. Eng. 47 (2008) 2052–2054, https://doi.org/10.1002/anie.200704313.